TECHNIQUES FOR ESTIMATING SELECTED PARAMETERS OF THE U.S. GEOLOGICAL SURVEY'S PRECIPITATION-RUNOFF MODELING SYSTEM IN EASTERN MONTANA AND NORTHEASTERN WYOMING

By Lawrence E. Cary

U.S. GEOLOGICAL SURVEY

Water-Resources Investigations Report 91-4068

Prepared in cooperation with the

U.S. BUREAU OF LAND MANAGEMENT

Helena, Montana
November 1991

U.S. DEPARTMENT OF THE INTERIOR

MANUEL LUJAN, JR., Secretary

U.S. GEOLOGICAL SURVEY

Dallas L. Peck, Director

For additional information
write to:

District Chief
U.S. Geological Survey
428 Federal Building
301 South Park, Drawer 10076
Helena, MT 59626-0076

Copies of this report can be
purchased from:

U.S. Geological Survey
Books and Open-File Reports Section
Federal Center, Bldg. 810
Box 25425
Denver, CO 80225-0425

CONTENTS

Page

Abstract 1
Introduction 2
  Purpose and scope. 3
  Previous investigations. 4
Study area 4
Model description. 5
Parameter selection. 7
Parameter-estimation techniques. 9
  Potential evapotranspiration 9
  Lapse rates. 16
  Vegetation 20
    Vegetation crown cover 20
    Vegetation rooting depths. 23
  Soils. 23
  Subsurface flow and base flow. 30
Summary. 33
References cited 36

ILLUSTRATIONS

Figure 1. Map showing location of study area 3
2. Schematic diagram of the Precipitation-Runoff Modeling System and its input variables. 6
3. Graphs showing initial isotropic and anisotropic empirical semivariograms of the air-temperature coefficient (CTS) and air-temperature correction coefficient (CTX) of the Jensen-Haise equation. 11
4. Graphs showing final empirical semivariograms of the air-temperature coefficient (CTS) and air-temperature correction coefficient (CTX) of the Jensen-Haise equation 13
5-8. Maps showing:
5. Regionalized values of the air-temperature coefficient (CTS) and associated error 14
6. Regionalized values of the air-temperature correction coefficient (CTX) and associated error 15
7. Location of climatological stations used in the computation of lapse rates for air temperature. 16
8. Location of streamflow-gaging stations used in determining subsurface-flow and base-flow recession. . . . 31

TABLES

Table 1. Parameters selected for estimation 8
2. Climatological stations used in the computation of lapse rates for air temperature. 17
3. Monthly mean lapse rates for maximum air temperature (TLX) 18
4. Monthly mean lapse rates for minimum air temperature (TLN) 19
5. Coefficients of variation in lapse rates for maximum (TLX) and minimum (TLN) air temperatures 20
6. Total crown cover within major vegetation types and dryland crops, by landform 21
7. Crown cover identified by growth form within major vegetation types, by landform 22
8. Rooting depths and soil-texture class occurrence of major vegetation types and dryland crops, by landform. 24
9. Summary of the regression analyses of selected properties for undisturbed soil samples 26
10. Soil-texture classes represented in the soil samples used in the analyses. 28

TABLES--Continued

Page

Table 11. Relative error between measured soil properties and estimates made using the regression equations from table 9. 29
12. Streamflow-gaging stations used in the study of subsurface-flow and base-flow recession. 32

CONVERSION FACTORS AND VERTICAL DATUM

Multiply	By	To obtain
bar	100	kilopascal
cubic foot per second	0.028317	cubic meter per second
Fahrenheit degrees per 1,000 feet (F°/1,000 ft)	1.823	Celsius degrees per 1,000 meters
foot (ft)	0.3048	meter
inch (in.)	25.4	millimeter
inch per day (in/d)	25.4	millimeter per day
inch per hour (in/h)	25.4	millimeter per hour
inch per square mile	9.807	millimeter per square kilometer
mile (mi)	1.609	kilometer
millibar	100	pascal
square mile (mi^2)	2.59	square kilometer

Temperature can be converted from degrees Fahrenheit (°F) to degrees Celsius (°C) by the equation:

$$°C = 5/9 (°F - 32)$$

Sea level: In this report "sea level" refers to the National Geodetic Vertical Datum of 1929--A geodetic datum derived from a general adjustment of the first-order level nets of the United States and Canada, formerly called Sea Level Datum of 1929.

TECHNIQUES FOR ESTIMATING SELECTED PARAMETERS OF THE U.S. GEOLOGICAL SURVEY'S PRECIPITATION-RUNOFF MODELING SYSTEM IN EASTERN MONTANA AND NORTHEASTERN WYOMING

By Lawrence E. Cary

ABSTRACT

This report describes techniques that can be used to estimate selected parameters of the U.S. Geological Survey's Precipitation-Runoff Modeling System when applied to eastern Montana and northeastern Wyoming. Techniques are described for estimating coefficients in a potential evapotranspiration equation, lapse rates for maximum and minimum air temperatures, vegetation crown cover, vegetation rooting depths, physical and hydrologic properties of soils, and subsurface-flow and base-flow routing coefficients.

Values of the two coefficients in a potential evapotranspiration equation were estimated at points by kriging. The air-temperature coefficient, in reciprocal degrees Fahrenheit, ranged from 0.0140 in the southwest corner of the study area to 0.0120 near the northern boundary. The air-temperature correction coefficient, in degrees Fahrenheit, ranged from 14.5 to about 18.5. The associated error in the estimated values did not exceed 4.0 percent.

Monthly mean lapse rates for maximum and minimum air temperatures were computed, then tested for differences between the mountains, the major river valleys, and the plains. The same monthly mean lapse rate for maximum air temperature can be used in all three areas. However, different lapse rates for minimum air temperature are needed in the mountains than in the valleys and plains. Lapse rates for maximum air temperature, in Fahrenheit degrees per 1,000 feet of elevation, were smallest in January (3.2) and largest in April and May (5.3). The lapse rate for minimum temperature, in the same units, was smallest in October (4.1) and largest in July (6.1) in the mountains. Minimum air-temperature lapse rates were generally smaller in the valleys and plains than in the mountains, and commonly were negative. They ranged from -1.8 Fahrenheit degrees per 1,000 feet in January to 2.5 Fahrenheit degrees per 1,000 feet in May. The error in estimating air temperature may be considerable when the lapse rates are used, especially in the valleys and plains.

Vegetation-crown-cover data were summarized from earlier studies. Crown cover was most extensive (mean of 63 percent) and least variable (coefficient of variation of 6 percent) in the riparian-woods type of vegetation. Crown cover was least extensive (mean of 24 percent) and most variable (coefficient of variation of 71 percent) in the ponderosa-pine type. When summarized by growth form, crown cover of shrubs was most extensive (mean of 29 percent) in the silver-sagebrush-grassland type and least extensive (mean of 2 percent) in the mixed-grassland type. The crown cover of shrubs was most variable (coefficient of variation of 137 percent) in the riparian-woods type and least variable (coefficient of variation of 14 percent) in the mixed-grassland type on uplands. Crown cover of grasses and forbs was most extensive (mean of 59 percent) and least variable (coefficient of variation of 14 percent) in the riparian-woods type. Crown cover of grasses and forbs was least extensive (mean of 23 percent) and most variable (coefficient of variation of 100 percent) in the greasewood type.

Vegetation rooting depths were summarized from soil profiles described in previous studies. The rooting depths were deepest (mean of 48 inches) and least variable (coefficient of variation of 19 percent) in the riparian-woods type. The rooting depths were shallowest in the ponderosa-pine type (mean of 24 inches) and in the breaks (mean of 19

inches). The rooting depths were most variable (coefficient of variation of 66 percent) in the greasewood type.

Estimating equations were developed between several physical and hydrologic properties of soils to which model parameters are related and the properties that commonly are measured. Parameters that can be estimated are maximum snowmelt-infiltration rate of the soil profile at field capacity, seepage rate from the soil-zone reservoir to the ground-water reservoir, maximum soil-moisture storage in the soil-zone reservoir and the recharge zone, hydraulic conductivity at the wetting front, the product of moisture deficit at field capacity and suction at the wetting front, the product of moisture deficit at the wilting point and suction at the wilting point divided by the product of moisture deficit at field capacity and suction at the wetting front, and a coefficient for redistribution of moisture from saturated storage to the recharge zone. The error that can be expected when values are estimated from the equations ranged from small for bulk density (coefficient of variation of 5.9 percent) to large for saturated hydraulic conductivity (coefficient of variation of 131 percent).

The subsurface-flow and base-flow routing coefficients are related to computed recession constants of a hydrograph. Mean recession constants were determined for streams in the study area having drainage areas of 100 square miles or less. Estimating equations for the subsurface-flow and base-flow recession constants were developed. The subsurface-flow recession constant can be estimated from the longitude and drainage area of the gaging station (coefficient of determination of 60 percent). The base-flow recession constant can be estimated from mean annual streamflow and mean annual precipitation (coefficient of determination of 63 percent).

INTRODUCTION

Interest in the water resources of semiarid regions has increased in recent years. Interest is particularly intense in the semiarid regions of eastern Montana and northeastern Wyoming, where coal deposits are being surface mined. Watershed models are being considered as mechanisms to (1) extend streamflow records, (2) simulate the hydrology of ungaged basins, and (3) simulate changes in hydrology due to changes in land use.

The U.S. Geological Survey has developed a watershed model known as the Precipitation-Runoff Modeling System (PRMS) (Leavesley and others, 1983). The model simulates components that are important identifiers of the hydrologic properties of watersheds. These hydrologic components are represented by equations that have either a theoretical or an empirical basis.

PRMS contains 45 parameters in the continuous or daily mode and 15 in the storm mode. The set of values for these parameters that would produce similar simulated flows is probably large. The number of parameters probably exceeds the number that can be fitted using objective optimization techniques (see, for example, Overton and Meadows, 1976, p. 11-13). In addition, the model may be more sensitive to some parameters than to others, depending on local conditions and watershed characteristics. The parameters to which the model results are not particularly sensitive can be excluded from optimization procedures to decrease the number to a manageable level. Physical parameters that can be measured or estimated accurately also can be excluded from optimization procedures.

Increasing the number of parameters that could be estimated from data would decrease the number of parameters that would have to be optimized, making application of PRMS to watersheds with limited data more feasible. Accordingly, the U.S. Geological Survey, in cooperation with the U.S. Bureau of Land Management, conducted this study of parameter-estimation techniques.

Purpose and Scope

This report describes techniques that can be used to estimate selected parameters in PRMS. Techniques are described for estimating coefficients in a potential evapotranspiration equation, lapse rates for maximum and minimum air temperatures, vegetation crown cover, vegetation rooting depths, physical and hydrologic properties of soils, and subsurface-flow and base-flow routing coefficients. The techniques are applicable to eastern Montana and northeastern Wyoming (fig. 1).

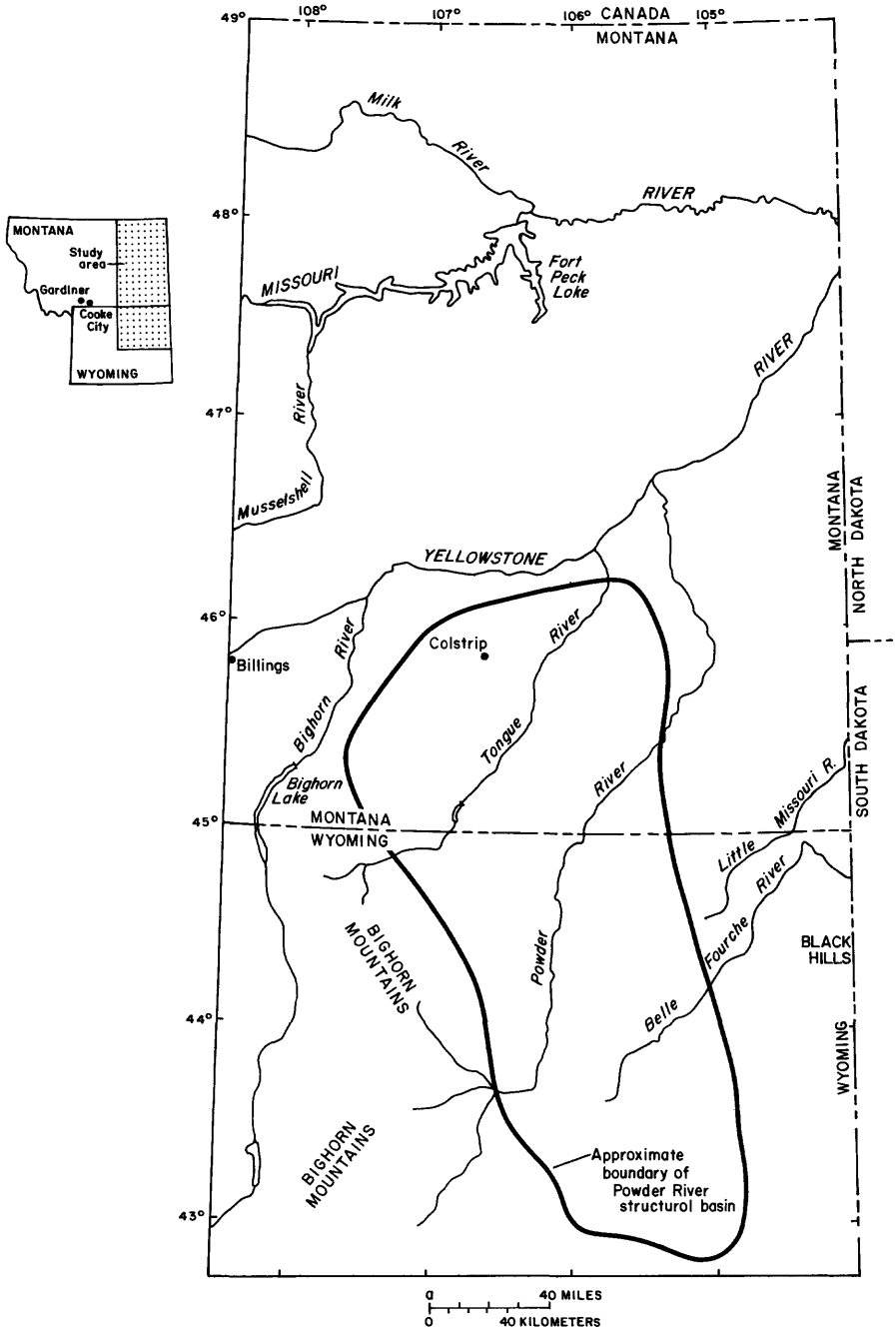

Figure 1.--Location of study area.

Data were acquired from various sources. Published air-temperature data from National Weather Service climatological stations in and near the study area were used to compute the coefficients in a potential evapotranspiration equation and the lapse rates for air temperature. Vegetation crown-cover and rooting-depth data were obtained from published reports. Soil data were obtained from files of the U.S. Geological Survey and published reports. Streamflow data, used in estimating the subsurface-flow and base-flow routing coefficients, were obtained from water-resources-data reports for Montana, Wyoming, and North Dakota.

Several statistical methods were applied. Kriging was used to interpolate coefficients in the evapotranspiration equation. T-tests were used in testing for differences in lapse rates between the mountains, major river valleys, and plains. Linear and multiple linear regressions were used to develop the estimating equations for physical and hydrologic properties of soils and for the subsurface-flow and base-flow routing coefficients.

Previous Investigations

PRMS is described in detail by Leavesley and others (1983). Examples of the use of PRMS are cited by Leavesley (1973), Weeks and others (1974), Leavesley and others (1981), and Scott (1984). The results of testing the daily and storm modes, including parameter optimization and sensitivity analysis for a watershed in southeastern Montana, were included in a report of Cary (1984). The reader can consult these references for a description of the model, its operation, and its application.

STUDY AREA

The study area includes eastern Montana and northeastern Wyoming. The area encompasses about 90,000 mi^2, including the Powder River structural basin (fig. 1), in the northern Great Plains physiographic province. The study area extends from the eastern borders of Montana and Wyoming to 108° 30′ west longitude, and from 42° 45′ to 49° north latitude. The topography ranges from gently rolling plains to rugged terrain, and the land-surface elevation generally decreases toward the north and east.

Most of the area is underlain by the Fort Union Formation (Paleocene age); however, surficial deposits in the south-central part of the Powder River structural basin consist of the overlying Wasatch Formation (Eocene age). Lithology of these formations is principally sandstone, siltstone, claystone, and coal beds. Burning of the coal beds has resulted in extensive areas of clinker in many parts of the region. Other sedimentary-rock formations crop out in the foothills bordering the Black Hills and the Bighorn Mountains in Wyoming and along the west and north sides of the study area in Montana, as well as along mountain flanks. Keefer (1974) compiled a general geologic map of the region, which can be consulted for the location and areal extent of the surface formations.

The climate in the region is semiarid, with hot summers and cold winters (Northern Great Plains Resources Program, 1974, p. 45). The mean January temperature is about 28 °F, whereas the mean July temperature is about 88 °F. Precipitation ranges from 10 to 16 in. on the plains. Sixty percent of the precipitation occurs from May through September. Much of the rest occurs as snow during late fall, winter, and early spring. Most storms during the fall, winter, and spring are cyclonic. During the summer, convective storms are common.

The major vegetation types and soil associations in the northern Great Plains are shown on a map by the Northern Great Plains Resources Program (1974, pl. 7). Eleven vegetation types and about 20 major soil associations are identified on the map for this region. Vegetation types include mixed grassland (mid and short grasses), sagebrush-grassland (predominantly big and silver sagebrush), greasewood, ponderosa pine, riparian woods, and breaks. Eighty-four percent of the area contains grass or sagebrush vegetation (Northern Great Plains Resources Program, 1974, p. 48, 51). Soil characteristics vary considerably, depending upon parent material and other soil-forming factors.

Seventy percent of the area is rangeland and 26 percent is cultivated. About 3 percent of the area is irrigated. Most of the cultivated land is used for wheat production (Northern Great Plains Resources Program, 1974, p. 45).

MODEL DESCRIPTION

PRMS is described briefly in the following paragraphs. The reader can refer to Leavesley and others (1983) for a complete description.

PRMS is a deterministic, physical-process model that simulates the hydrologic processes that are active in a basin. Each process is simulated by a mathematical expression that either is based on known physical laws or is an empirical expression with some physical interpretation. The constants, coefficients, and exponents in these expressions form the model parameter set for which estimates need to be provided by the user. Sixty parameters can be optimized and subjected to sensitivity analysis using algorithms provided in the model.

PRMS has two simulation modes--daily and storm. PRMS can be operated as a distributed-process model or a lumped-process model. When operated as a distributed-process model in the daily mode, a modeled basin is divided into hydrologic response units. Hydrologic response units are delineated using basin geology, vegetation types, soil types, slope, aspect, climate, elevation, and land use. In the storm mode, a modeled basin is divided into overland-flow planes interconnected by channel segments. A hydrologic response unit is equivalent to one or more overland-flow planes. When operated as a lumped-process model, spatial variability is ignored, and a modeled basin is considered to be composed of one hydrologic response unit or two overland-flow planes and one channel segment.

A schematic diagram of PRMS is provided in figure 2. Model input variables include air temperature, precipitation (rain, snow, or mixed rain and snow), and solar radiation. Part of the precipitation falling on a basin is intercepted and retained by the vegetation canopy. The remainder (net precipitation) reaches the land surface. Air temperature and solar radiation are the variables that drive the processes of evaporation, sublimation, transpiration, and snowmelt. The basin is conceptualized as a series of reservoirs in PRMS. The reservoirs are represented by rectangles in figure 2. The reservoirs include interception, the snowpack, an impervious zone, a soil zone, the subsurface, and ground water. Model output variables from the reservoirs include return of water vapor to the atmosphere, seepage to ground water, surface flow, and seepage to streamflow, which are combined to form the model's response.

In the daily mode, intercepted precipitation is returned to the atmosphere by evaporation or sublimation. If the net precipitation is snow, it is added to the snowpack. Some of the snowpack is returned to the atmosphere by sublimation, and the remainder melts and infiltrates into the soil-zone reservoir. When the soil reaches field capacity, snowmelt in excess of a maximum infiltration rate becomes surface flow.

Net rainfall is apportioned between surface flow from part of each hydrologic response unit and infiltration on the remainder of each hydrologic response unit. The surface flow is computed using a contributing-area concept.

Both rain and snowmelt can occur on an impervious area. Any water in excess of the retention storage capacity of the impervious area becomes surface flow. The water in retention storage is evaporated.

The soil-zone reservoir is divided into recharge and lower zones. Water in excess of storage capacity of the recharge zone flows to the lower soil zone. Water in excess of the storage capacity of the lower soil zone flows out of the zone. Water can be returned to the atmosphere by evapotranspiration (combination of evaporation from the soil and transpiration by plants) from the recharge zone, and by transpiration from the lower soil zone.

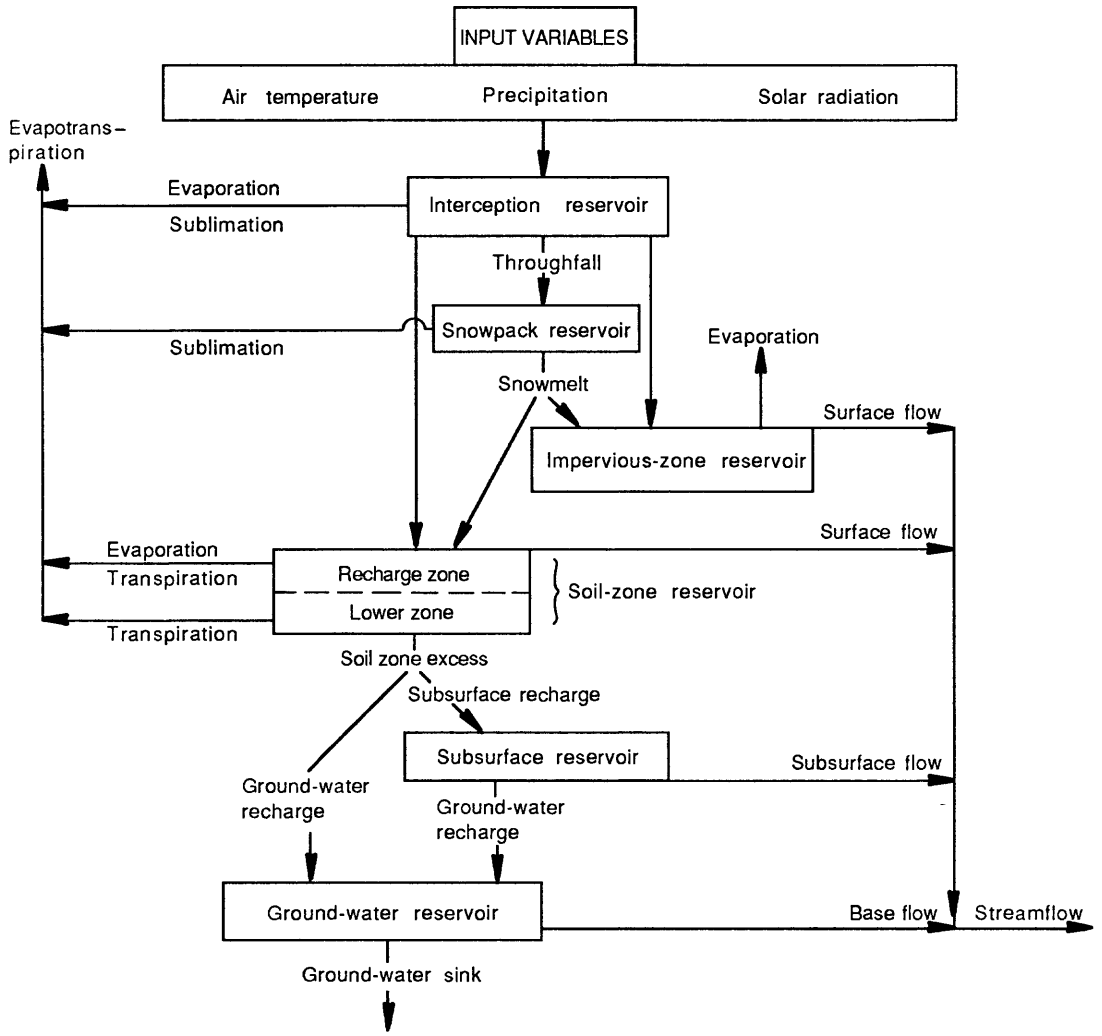

Figure 2.--Schematic diagram of the Precipitation-Runoff Modeling System and its input variables (modified from Leavesley and others, 1983, p. 8).

Water leaving the soil-zone reservoir is apportioned between a ground-water reservoir and a subsurface reservoir using a maximum daily ground-water recharge value. Water in excess of the maximum daily recharge value flows into an associated subsurface reservoir. The subsurface reservoir represents water that is available in the saturated and unsaturated zones for relatively rapid movement to stream channels. Part of the water in this reservoir moves to the stream channel as subsurface flow. The remainder seeps to the ground-water reservoir.

Water can move from the ground-water reservoir in two ways. Part of the water can be released to the stream channel as base flow. Water also can seep from the ground-water reservoir to a ground-water sink.

Daily mean streamflow at the basin outlet is computed as the sum of surface flow from each hydrologic response unit, subsurface flow from each subsurface reservoir, and base flow from each ground-water reservoir. If lakes are present in the basin, the flow can be routed through them before reaching the basin outlet.

In the daily mode, model output includes daily mean streamflow, the daily contents of each conceptual reservoir, the quantity of water lost from the basin to

the atmosphere, and seepage to the ground-water sink. Monthly and annual summaries also can be computed.

In the storm mode, net rainfall is allocated to infiltration and rainfall excess during snow-free periods. A point infiltration capacity is computed. The point infiltration capacity changes for each succeeding time interval during the storm, depending on the quantity of water stored in the recharge zone. Net infiltration is next computed by assuming that it varies linearly from zero to a maximum equal to the current point infiltration capacity. The rainfall that has infiltrated is added to recharge-zone storage and is used to update the point infiltration capacity. During rainfree periods of a storm, soil moisture in the recharge zone can seep to the lower soil zone and be decreased by evaporation. When the storage capacity of the lower soil zone is exceeded, the excess is routed to the subsurface or ground-water reservoirs in the same way it is routed in the daily mode.

Rainfall excess is computed as the difference between net rainfall and infiltration. The rainfall excess is routed as surface flow over the overland-flow planes to the channel segments, then down each channel segment to the basin outlet. If reservoirs are present in the basin, one of two reservoir-routing techniques can be selected to route channel flow through the reservoirs.

The storm simulation mode also has an optional sediment-routing capability. Sediment is detached from the overland-flow planes and routed to the channel segments, then through the segments to the basin outlet. The overland-flow and channel-flow variables for water required in the sediment-transport relations are obtained from the water-routing relations.

When the storm mode is used, the output includes the results of the daily simulation and the results of the simulation of each storm. The storm simulation results are the storm hydrograph, storm peak discharges, and storm volumes. If the sediment-routing option is used, the concentration and total quantity of sediment reaching the outlet are computed.

PARAMETER SELECTION

Estimation techniques developed in this study are for parameters to which PRMS results were determined to be sensitive. The results of a study of a small basin in southeastern Montana (Cary, 1984) and of a small basin in northwestern Colorado (Leavesley and others, 1981) were used to aid in parameter selection. Some parameters to which the model is sensitive were not included because they have strong physical interpretation and have values that were assigned as the result of previous investigations.

Parameters selected for estimation are related to climate, vegetation, soils, and streamflow; all are considered in the daily mode of PRMS except four characterizing the soil zone that are considered in the storm mode. All parameters selected for study are defined in table 1. Those related to climate are two coefficients used in calculating potential evapotranspiration and the lapse rates for maximum and minimum air temperature. The parameters related to vegetation are vegetation crown (canopy) cover for summer and winter. Parameters used to characterize the soil-zone reservoir can be estimated from vegetation rooting depths and various physical and hydrologic properties of soils. Those parameters, in the daily mode, are maximum snowmelt-infiltration rate, seepage rate from the soil-zone reservoir to a ground-water reservoir, and maximum soil-moisture storage in the soil-zone reservoir and in the recharge zone. Those in the storm mode are hydraulic conductivity at the wetting front, a coefficient that is the product of moisture deficit at field capacity and suction at the wetting front (matric suction), a coefficient that is the product of moisture deficit at the wilting point and suction at the wetting front divided by the product of moisture deficit at field capacity and suction at the wetting front, and a coefficient for seepage from the saturated part of the soil-zone reservoir to the recharge zone. Finally, contributions to streamflow from the subsurface and ground-water reservoirs are controlled by a subsurface-flow routing coefficient and a base-flow routing coefficient in the daily mode.

Table 1.--*Parameters selected for estimation*

[°F, degrees Fahrenheit; HRU's, hydrologic response units; F°/1,000 ft, Fahrenheit degrees per 1,000 feet; in., inches; in/d, inches per day; in/h, inches per hour]

Parameter	Number of values	Definition	Mode
CTS	12 (monthly)	Air-temperature coefficient in a potential evapotranspiration equation ($°F^{-1}$)	Daily
CTX	No. of HRU's	Air-temperature correction coefficient in a potential evapotranspiration equation (°F)	Daily
TLX	12 (monthly)	Lapse rate for maximum air temperature, by month (F°/1,000 ft)	Daily
TLN	12 (monthly)	Lapse rate for minimum air temperature, by month (F°/1,000 ft)	Daily
COVDNS	No. of HRU's	Vegetation crown cover during summer (decimal fraction)	Daily
COVDNW	No. of HRU's	Vegetation crown cover during winter (decimal fraction)	Daily
SRX	No. of HRU's	Maximum snowmelt-infiltration rate of soil profile at field capacity (in.)	Daily
SEP	No. of HRU's	Seepage rate from soil-zone reservoir to ground-water reservoir (in/d)	Daily
SMAX	No. of HRU's	Maximum soil-moisture storage in the soil-zone reservoir (in.)	Daily
REMX	No. of HRU's	Maximum soil-moisture storage in the recharge zone (in.)	Daily
KSAT	No. of HRU's	Hydraulic conductivity at the wetting front (in/h)	Storm
PSP	No. of HRU's	Coefficient that is the product of moisture deficit at field capacity and suction at the wetting front (in.)	Storm
RGF	No. of HRU's	Coefficient that is the product of moisture deficit at wilting point and suction at the wetting front divided by the product of moisture deficit at field capacity and suction at the wetting front (dimensionless)	Storm
DRN	No. of HRU's	Coefficient for redistribution of moisture from saturated storage to the recharge zone (in/h)	Storm
RCF	No. of subsurface reservoirs	Subsurface-flow routing coefficient (decimal fraction)	Daily
RCB	No. of ground-water reservoirs	Base-flow routing coefficient (decimal fraction)	Daily

PARAMETER-ESTIMATION TECHNIQUES

Even though parameters with physical significance can be estimated, a large degree of uncertainty may be involved. The inherent variability in vegetation and soils, for example, can affect the estimate. Data availability and reliability can also affect the estimation methods and their results. The techniques used for parameter estimation vary with the parameter being studied and the information that is available.

Potential Evapotranspiration

Three methods are available for computing potential evapotranspiration in PRMS. The only method considered here is the modified Jensen-Haise equation (Jensen and others, 1969, p. 10), which is:

$$PET = CTS\ (TAVF - CTX)\ RIN \quad (1)$$

where

PET = potential evapotranspiration, in inches per day;
CTS = air-temperature coefficient for a given area, in reciprocal degrees Fahrenheit;
TAVF = mean daily air temperature, in degrees Fahrenheit;
CTX = air-temperature correction coefficient for a given area, in degrees Fahrenheit; and
RIN = incident solar radiation, in equivalent depth of evaporation, in inches per day.

Jensen and others (1969, p. 10) indicate that, in the absence of calibrating evapotranspiration data, CTS and CTX can be estimated using data for the month with the highest mean temperature. For vegetation types in the study area, these coefficients are estimated as (Jensen and others, 1969):

$$CTS = \frac{1}{C1 + 13\ CH} \quad (2)$$

where

$$C1 = \text{elevation correction factor} = 68 - \frac{3.6\ E}{1{,}000}; \quad (3)$$

$$CH = \text{humidity index} = \frac{50\ \text{millibars}}{e_2 - e_1}; \quad (4)$$

E = elevation of land surface, in feet above sea level;
e_2 = saturation vapor pressure, in millibars, at the mean maximum air temperature for the warmest month; and
e_1 = saturation vapor pressure, in millibars, at the mean minimum air temperature for the same month.

Also:

$$CTX = 27.5\ °F - \left[0.25\ (e_2 - e_1) - \frac{E}{1{,}000}\right] \quad (5)$$

CTS and CTX vary with air temperature (indirectly through vapor pressure) and thus are related to latitude. The variation with latitude would be particularly noticeable in the study area, which extends over more than 6 degrees of latitude. CTS can be expected to decrease at the more northerly latitudes, whereas CTX would increase.

Values of CTS and CTX were estimated by kriging, which is a method for interpolating values between points of known value. A brief description is given here. For a detailed description of the general characteristics of kriging, or for its use in a hydrologic context, the reader is referred to David (1977) or McCuen and Snyder (1986, p. 150-197), respectively.

In kriging, the best estimate at a point is assumed to be a weighted mean of all measured values within an area of influence surrounding the point. The radius of this area of influence (radius of influence) is defined by the distance between points beyond which the correlation between measured values is not significant.

An equation that describes the relation of the variance between measurement points and the separation distance (h) between measurement points is needed in kriging. The equation is used to compute the optimal values of the weights to be included in the weighted mean and the standard errors of estimate and to determine the radius of influence. The empirical semivariogram is a graph of the computed variances between measured values plotted against the separation distances. The theoretical semivariogram is the equation that best fits the empirical semivariogram. The separation distance at which the semivariogram approaches a constant value (the sill) is the radius of influence.

The empirical semivariogram might be affected by three factors that need to be considered when selecting a theoretical semivariogram. First, the measured values might display a regular change in value with direction (a trend). Where present, the trend needs to be removed from the measured values before further analysis. Second, in some instances the empirical semivariogram will not pass through the origin when the separation distance is zero, but will have some positive value (the nugget effect). This positive value is included in the theoretical semivariogram as an additional parameter to improve the goodness of fit. Third, pairs of measured values with a certain orientation might display larger correlation than pairs with other orientations. The theoretical semivariogram will then be a function of direction as well as distance.

Temperature stations were selected in eastern Montana and northeastern Wyoming in such a way that the foothills and plains in the study area were represented. July temperature data for 1972-81 were obtained from the National Oceanic and Atmospheric Administration (1972-81a and 1972-81b). Values of CTS and CTX were computed using equations 2 and 5 and mean values of maximum and minimum air temperatures.

The empirical semivariograms for CTS and CTX were constructed, using the southwest corner of the study area as the origin. Because the climatological stations are irregularly spaced, distance intervals were used. The study area included about 6 1/2 degrees of latitude and about 4 1/4 degrees of longitude, so trends in measured values would be likely. Semivariograms were constructed for measured values oriented north-south (N-S), east-west (E-W), northwest-southeast (NW-SE), and northeast-southwest (NE-SW) (anisotropic semivariograms), and were constructed without regard to orientation (isotropic semivariograms). The empirical semivariograms for CTS and CTX are shown in figure 3. The plots do not extend to the vertical axis because the shortest distance between climatological stations was about 20 mi.

The parabolic shape of the semivariograms (fig. 3) indicates linear trend (David, 1977, p. 267). The linear trend is described by changes in the mean values of the measurements with direction. The mean values are modeled by a mean value function involving monomials in the X and Y directions (Skrivan and Karlinger, 1980, p. 13). First-degree polynomials in distance east (X direction) and distance north (Y direction) from the origin were found to adequately describe the trend.

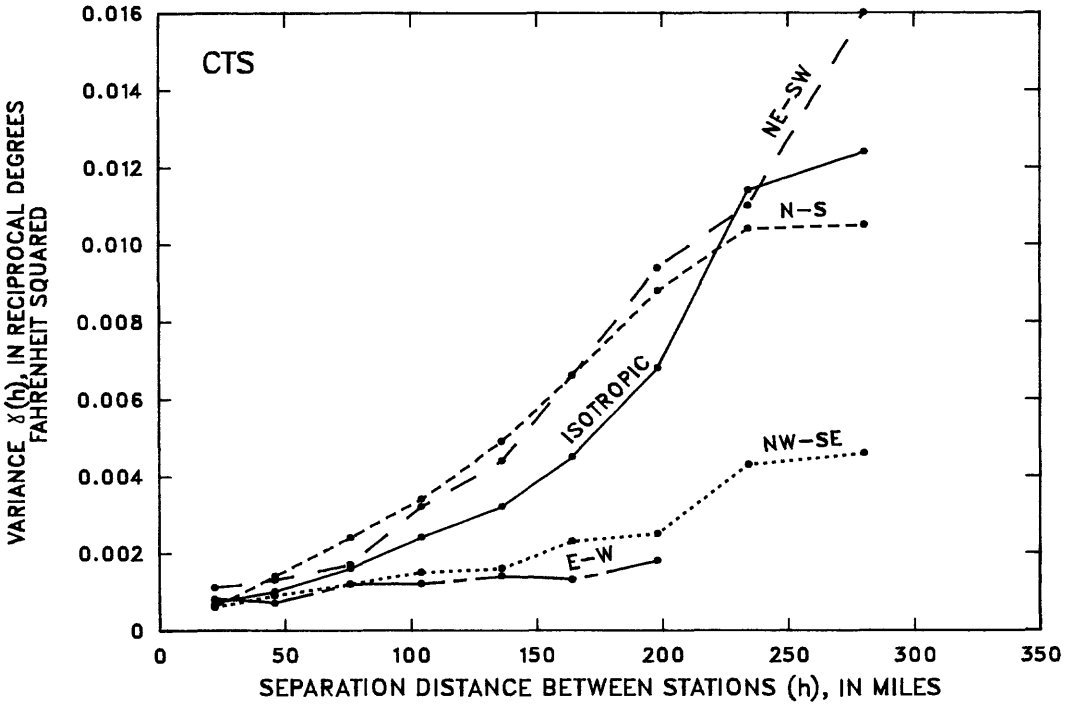

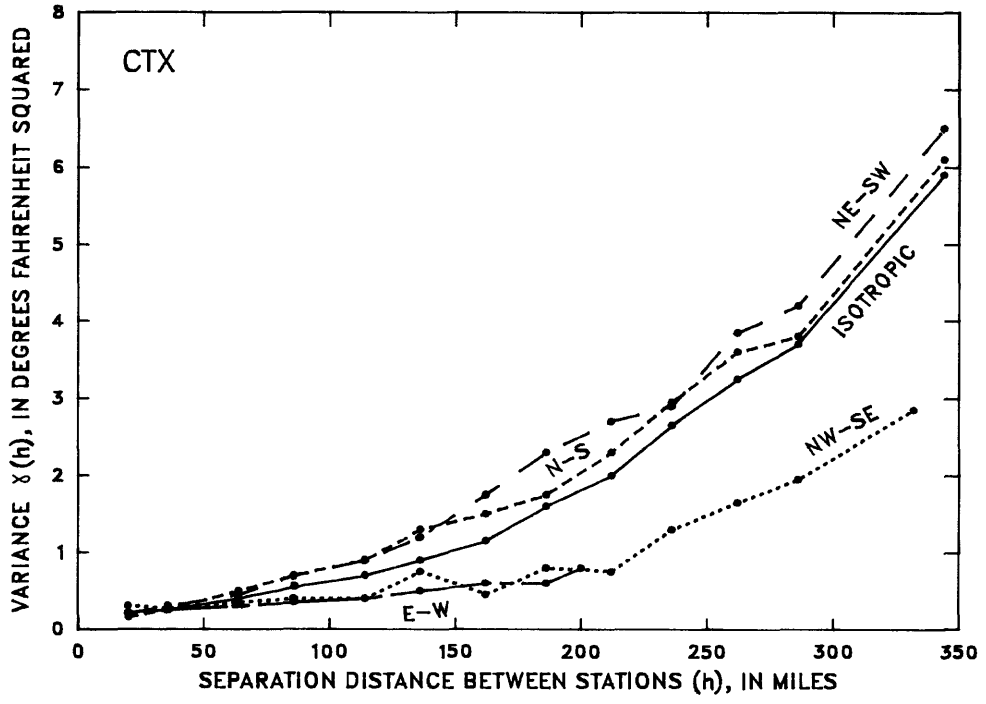

Figure 3.--Initial isotropic and anisotropic empirical semivariograms of the air-temperature coefficient (CTS) and air-temperature correction coefficient (CTX) of the Jensen-Haise equation (Jensen and others, 1969).

The equations were:

$$M_{CTS}(X,Y) = 0.0142 - (2 \times 10^{-6})\ X - (5 \times 10^{-6})\ Y, \text{ and} \quad (6)$$
$$M_{CTX}(X,Y) = 14.10 + (4.4 \times 10^{-3})\ X + (1 \times 10^{-2})\ Y \quad (7)$$

where

$M_{CTS}(X,Y)$ = mean value of CTS, in reciprocal degrees Fahrenheit;
$M_{CTX}(X,Y)$ = mean value of CTX, in degrees Fahrenheit;
X = distance east of origin, in miles; and
Y = distance north of origin, in miles.

CTS and CTX display anisotropy, which is greatest along the northeast-southwest direction (fig. 3). The semivariograms of CTS and CTX, therefore, are not functions of the separation distance between points alone, but functions of the separation distance and direction between points.

The final empirical semivariograms for CTS and CTX were constructed using measured values that had been adjusted for trends and considering the orientation of pairs of points. The measured values were adjusted for trends by subtracting the mean value for each point, where the mean value was computed from equations 6 and 7. Direction was included in the computations by giving greater weights to the pairs of points with northeast-southwest orientation. The final empirical semivariograms for CTS and CTX are shown in figure 4.

The sill is 0.0009 $°F^{-2}$ for CTS and 0.27 $°F^2$ for CTX (fig. 4). These values occur at a radius of influence of about 68 mi. The theoretical semivariogram will increase to 68 mi and assume a constant value, equal to the sill, beyond 68 mi. Because there is an apparent nugget effect, the semivariograms also include a constant equal to the indicated intercept of the vertical axis.

Beyond the radius of influence, the fluctuations in the semivariogram are usually considered to be due to sampling errors. However, on some semivariograms, distinct patterns may occur because of areas showing negative correlations between stations or other regional structures. In these instances, a second increase in the semivariograms begins at about 220 to 230 mi. Why the increase occurs is not clear (and could be the subject of further study). M.R. Karlinger (U.S. Geological Survey, oral commun., 1983) has indicated that beyond this point, a regional effect may be dominant over the local correlation between stations.

Three theoretical semivariograms were evaluated--linear, exponential, and spherical. None of the three demonstrated a clear superiority to the others. The information was insufficient to determine the shape and response near the origin of the empirical semivariogram, so a linear model was adopted. The linear semivariogram for CTS, in reciprocal degrees Fahrenheit squared, was:

$$\gamma(h) = 4.41 \times 10^{-6}\ h + 6 \times 10^{-4} \text{ for values of h between 0 and 68 mi, and} \quad (8)$$
$$= 9 \times 10^{-4} \text{ for values of h greater than 68 mi,}$$

and for CTX, in degrees Fahrenheit squared, was:

$$\gamma(h) = 1.32 \times 10^{-3}\ h + 0.18 \text{ for values of h between 0 and 68 mi, and} \quad (9)$$
$$= 0.27 \text{ for values of h greater than 68 mi,}$$

where

$\gamma(h)$ = variance, and
h = separation distance between stations, in miles.

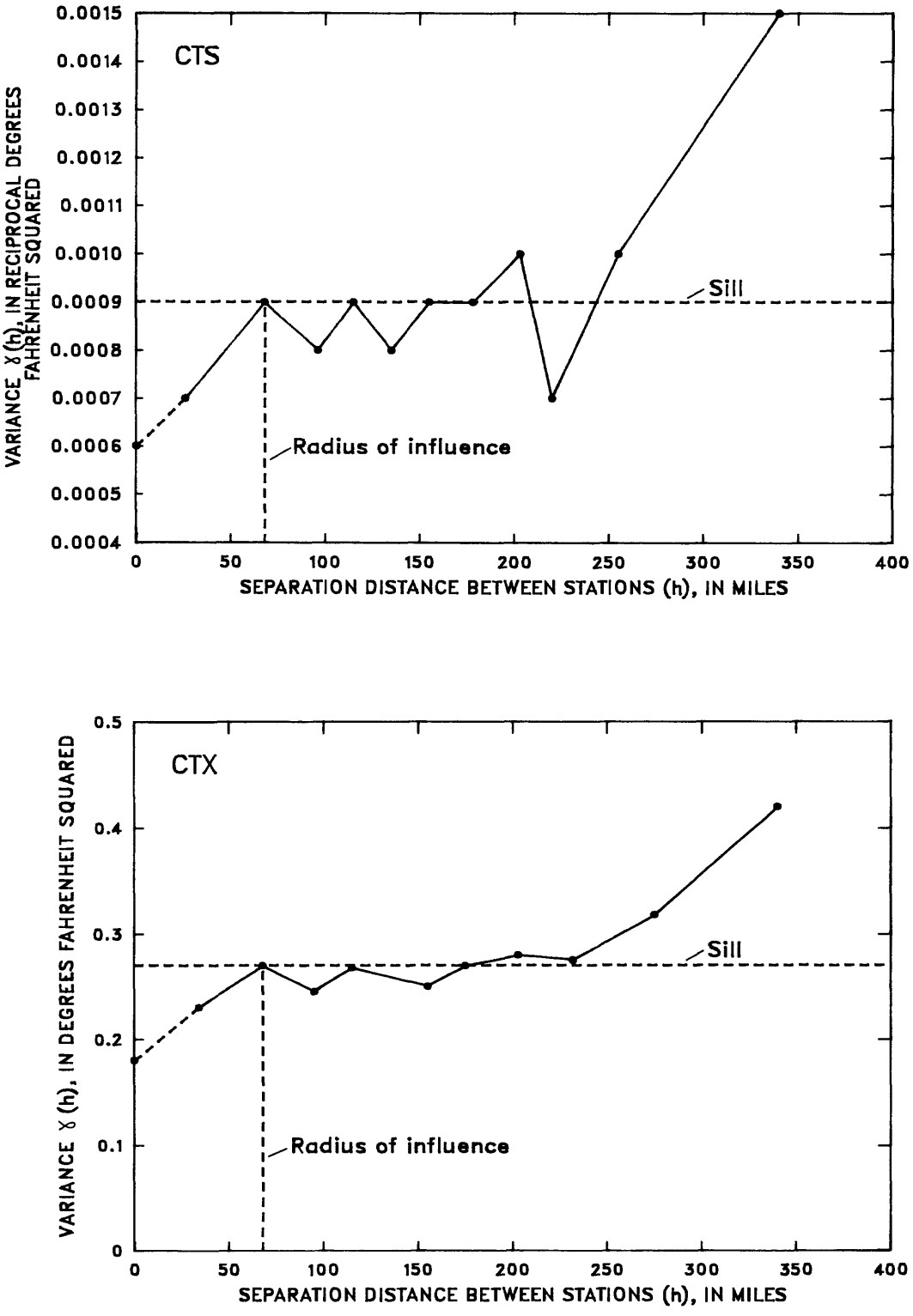

Figure 4.--Final empirical semivariograms of the air-temperature coefficient (CTS) and air-temperature correction coefficient (CTX) of the Jensen-Haise equation (Jensen and others, 1969).

Regionalized values of CTS and CTX, determined by kriging, are shown in figures 5 and 6, respectively. These maps can be used to estimate CTS and CTX at any point in the plains region of the study area where site data are not available. Estimates of CTS range from 0.0140 $°F^{-1}$ in the southwest corner of the region to 0.0120 $°F^{-1}$ in the north (fig. 5). The estimated values most likely will be in error by

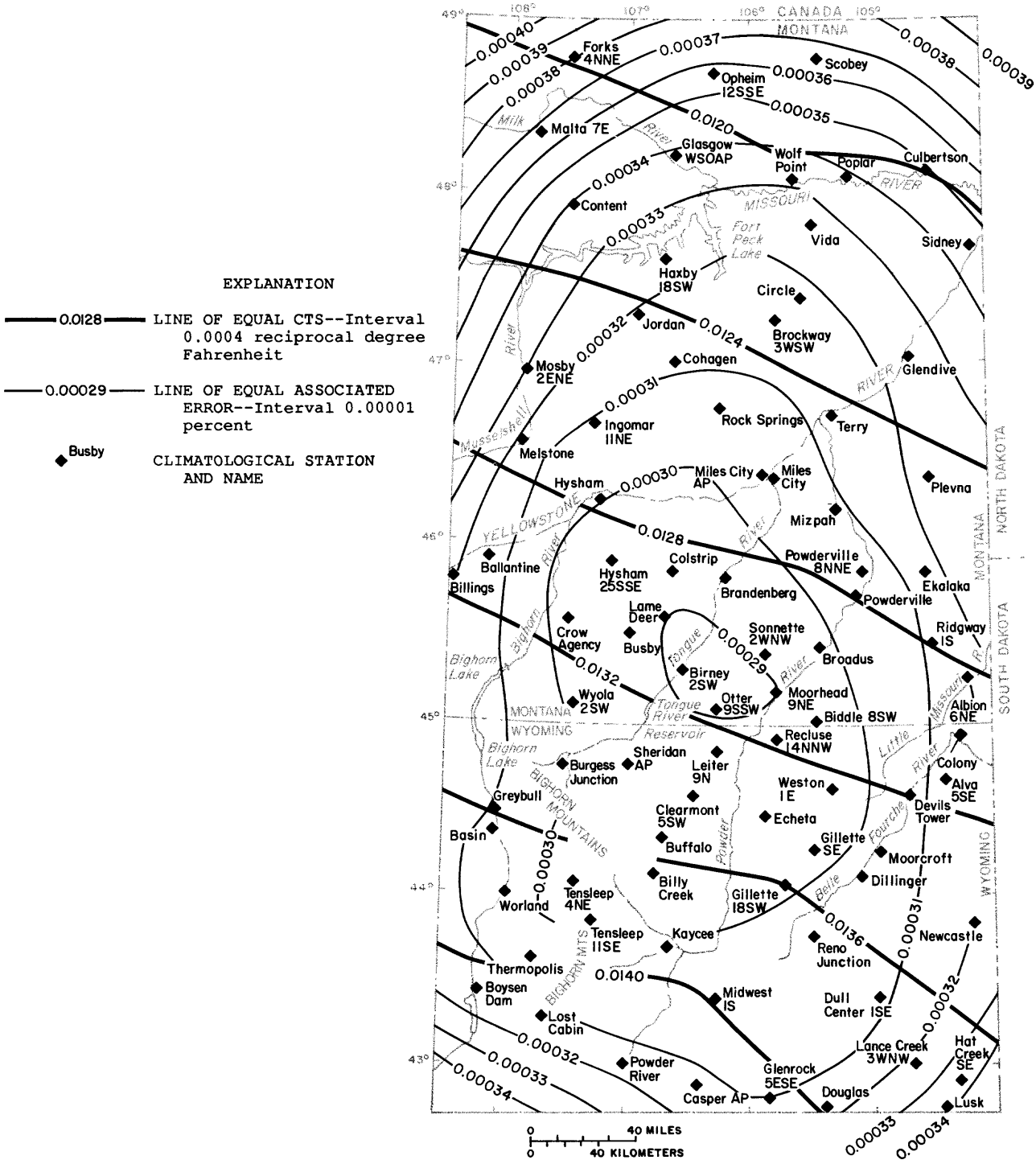

Figure 5.--Regionalized values of the air-temperature coefficient (CTS) and associated error.

no more than 2.4 percent (error divided by estimate multiplied by 100) in the southwest corner, increasing to 3.3 percent in the north. CTX increases northward, from 14.5 to about 18.5 °F (fig. 6). In a northward direction, the associated error decreases slightly from 4.0 to 3.2 percent then increases to 3.7 percent.

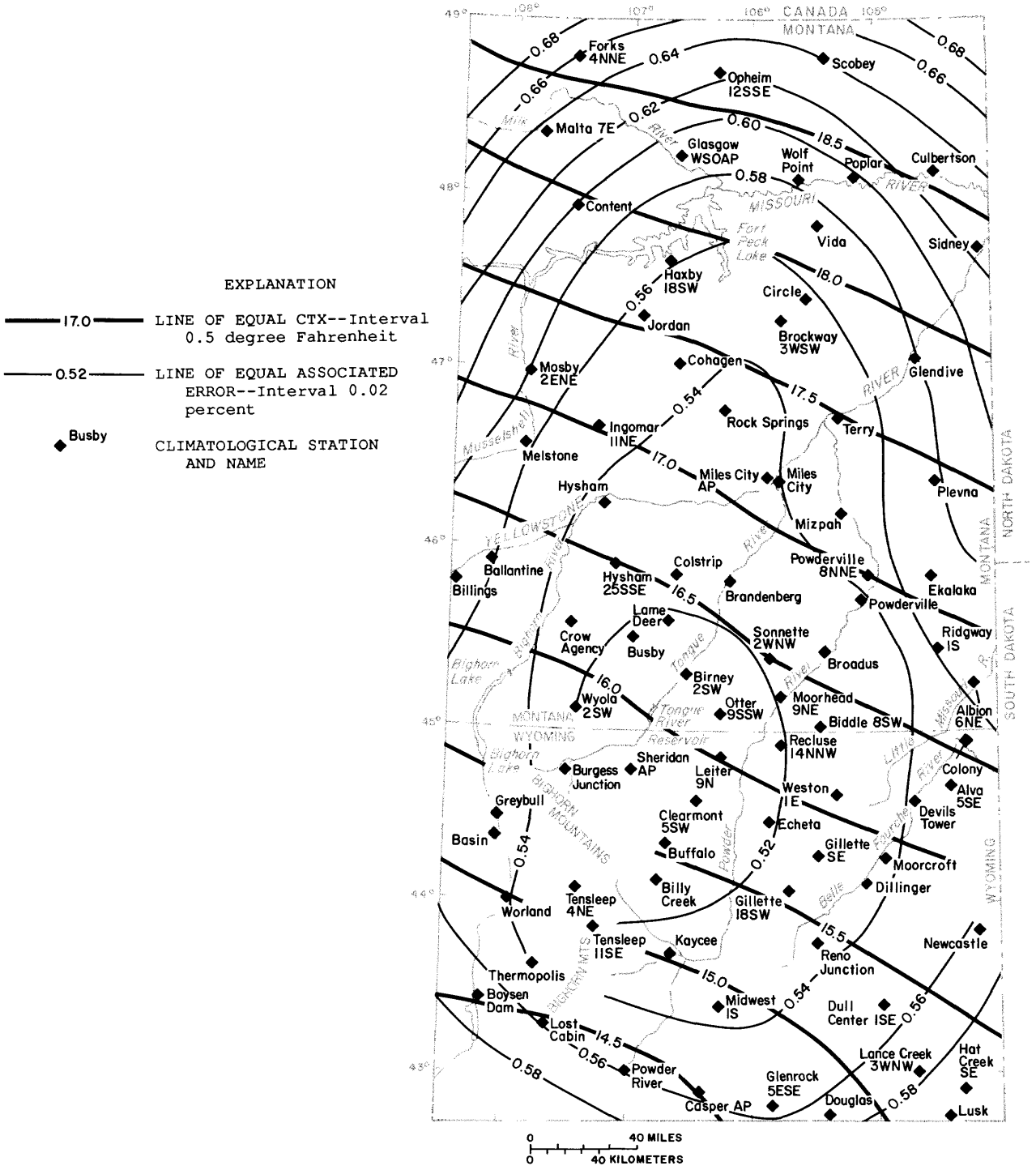

Figure 6.--Regionalized values of the air-temperature correction coefficient (CTX) and associated error.

Lapse Rates

Air temperature is important in the snowmelt and evapotranspiration components of PRMS. The importance of air temperature is reflected in the sensitivity of the model results to the lapse rates (change in temperature with change in elevation) for maximum daily temperature (TLX) and minimum daily temperature (TLN).

In the troposphere, the mean lapse rate for rising or falling airmasses is usually considered to be about 3.5 F°/1,000 ft. However, the actual lapse rate can differ from this mean value depending on local climate, season of the year, atmospheric moisture, and temperature (Weisner, 1970, p. 33). Owing to the possible variations and to model sensitivity, monthly mean lapse rates were investigated.

Plains, foothills, and river valleys, which commonly are bordered by rugged breaks, are present in the study area. The actual lapse rates may vary with location in the study area and with time. Therefore, lapse rates were compared, by month, for the mountains, the major river valleys, and the plains.

Climatological data for the analysis were obtained from reports of the U.S. Weather Bureau for Montana (1955, 1965a) and for Wyoming (1954, 1965b). Station pairs were selected for eastern and western flanks of mountain ranges, major river valleys, and the plains. The stations selected had 20 years of temperature data. Monthly mean maximum and mean minimum temperatures were computed for each station. Lapse rates between station pairs (a base station and a nearby station at a higher elevation) were computed as Fahrenheit degrees per 1,000 ft for mean maximum and mean minimum temperatures, for each month. The location of the stations used in the analysis is shown in figure 7. The National Weather Service climatological station names and elevations for each station are given in table 2.

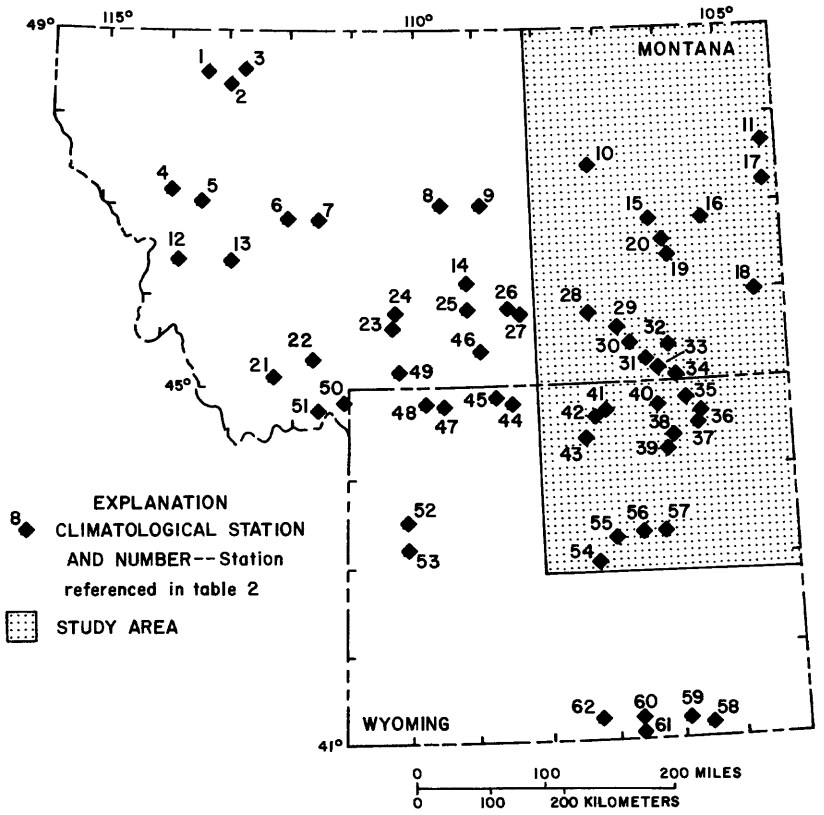

Figure 7.--Location of climatological stations used in the computation of lapse rates for air temperature.

Table 2.--*Climatological stations used in the computation of lapse rates for air temperature*

[Number in parentheses corresponds to station number in figure 7]

Base station	Companion station	Base station elevation above sea level (feet)	Companion station elevation above sea level (feet)
	East-Flank Mountains		
Clark 4 W (48)	Crandall Cr (47)	4,500	6,600
Centennial (60)	Foxpark (61)	8,074	9,060
Holter Dam (6)	Adel (7)	3,487	5,200
Browning (3)	Summit (2)	4,355	5,233
Livingston FAA AP (24)	Yellowstone NE Ent (49)	4,653	7,200
Red Lodge (46)	Yellowstone NE Ent (49)	5,575	7,200
Pinedale (52)	Kendall (53)	7,175	7,800
Buffalo (42)	Hunters Station (43)	4,645	7,400
	West-Flank Mountains		
Encampment 10 ESE (62)	Foxpark (61)	7,387	9,060
West Glacier (1)	Summit (2)	3,154	5,233
Ennis (22)	West Yellowstone (50)	4,953	6,665
Dillon AP (21)	Lakeview (51)	5,216	6,710
St. Ignatius (4)	Seeley Lake RS (5)	2,900	4,100
Hamilton (12)	Philipsburg RS (13)	3,529	5,270
Laramie (59)	Pole Mountain Nursery (58)	7,211	8,530
	Valleys		
Moorhead 9 NE (34)	Sonnette 2 WNW (32)	3,220	3,900
Arvada 3 N (40)	Recluse 3 NNE (35)	3,680	4,200
Birney 2 SW (30)	Otter 9 SSW (33)	3,190	4,100
Arvada 3 N (40)	Buffalo 5 W (41)	3,680	5,240
Lower Crazy Woman Cr (36)	Buffalo (42)	3,900	4,645
Billings WP (27)	Billings WSO AP (26)	3,655	4,125
Livingston (23)	Livingston FAA AP (24)	4,485	4,653
Lovell (44)	Deaver (45)	3,825	4,105
Birney 2 SW (30)	Kirby (31)	3,190	3,860
Savage (11)	Wibaux 2 E (17)	1,985	2,670
Columbus (25)	Rapelje 4 S (14)	3,585	4,125
Miles City (19)	Miles City FAA AP (20)	2,360	2,629
	Plains		
Gillette 2 E (38)	Gillette 18 SW (39)	4,556	4,903
Casper WB AP (54)	Midwest (55)	5,319	4,850
Dillinger (37)	Gillette 18 SW (39)	4,300	4,903
Midwest (55)	Ross (56)	4,850	5,250
Verse 8 NW (57)	Ross (56)	4,800	5,250
Grass Range (9)	Lewistown FAA AP (8)	3,480	4,125
Miles City FAA AP (20)	Rock Springs (15)	2,629	3,024
Jordan (10)	Rock Springs (15)	2,590	3,024
Mildred 5 N (16)	Ekalaka (18)	2,590	3,425
Crow Agency (28)	Busby (29)	3,030	3,500

Mean lapse rates for maximum and minimum air temperatures were tested for statistically significant differences (at the 0.10 significance level) using t-tests. Mean values were computed from the lapse rates between pairs of stations representing east-flank mountains, west-flank mountains, major river valleys, and plains. The mean lapse rates for west-flank mountains were tested against those for east-flank mountains. If differences were not statistically significant, all mountain lapse rates were combined and monthly mean values were computed. Next, the monthly mean lapse rates for valleys were tested against those for plains. Likewise, if differences were not statistically significant, the lapse rates for valleys and plains were combined and monthly mean values were computed. Next, the monthly mean lapse rates for valleys and plains were tested against those for mountains. If differences were not statistically significant, all the lapse rates were combined and a single, monthly mean value was computed for all station pairs.

Monthly mean lapse rates for maximum air temperature were tested first, and the results are summarized in table 3. No statistically significant differences were found between the east- and west-flank mountains or between the valleys and the plains. When the monthly mean values for the combined mountains and the combined valleys and plains were tested, significant differences in mean lapse rates were found for May and September. Because differences occurred in only 2 of 12 months, and because at the chosen significance level differences could be incorrectly identified 10 percent of the time, all the lapse rates were combined and a single value was computed for each month.

The monthly mean lapse rates for maximum air temperature displayed seasonal variation. The lapse rate was smallest in January (3.2 F°/1,000 ft), increasing to a maximum in April and May (5.3 F°/1,000 ft), and then decreasing through the remainder of the year.

Table 3.--*Monthly mean lapse rates for maximum air temperature (TLX)*

Stations	Sample size	Lapse rate, in Fahrenheit degrees per 1,000 feet											
		Jan	Feb	Mar	Apr	May	June	July	Aug	Sept	Oct	Nov	Dec
East-flank mountains	8	3.7	3.7	3.8	5.0	4.8	4.4	4.6	4.4	3.7	4.4	3.9	4.1
West-flank mountains	7	3.6 [1]	3.0 [1]	4.0 [1]	4.5 [1]	4.1 [1]	3.8 [1]	3.4 [1]	3.2 [1]	2.8 [1]	2.9 [1]	3.5 [1]	3.5 [1]
Valleys	12	2.0	3.6	5.6	5.6	6.2	5.4	4.6	4.6	4.8	4.6	2.5	2.1
Plains	10	3.6 [1]	5.4 [1]	5.9 [1]	6.0 [1]	6.2 [1]	5.6 [1]	6.0 [1]	6.4 [1]	5.7 [1]	5.8 [1]	4.6 [1]	4.1 [1]
Combined mountains	15	3.6	3.4	3.9	4.8	4.5	4.1	4.1	3.9	3.3	3.7	3.7	3.8
Combined valleys and plains	22	2.8 [1]	4.5 [1]	5.7 [1]	5.8 [1]	6.2 [2]	5.5 [1]	5.3 [1]	5.4 [1]	5.2 [2]	5.2 [1]	3.5 [1]	3.0 [1]
Combined mountains, valleys, and plains	37	3.2	3.9	4.8	5.3	5.3	4.8	4.7	4.6	4.2	4.4	3.6	3.4

[1] The two preceding values in the column were not significantly different.
[2] The two preceding values in the column were significantly different (at the 0.10 significance level).

Monthly mean lapse rates for minimum air temperature were tested next, and the results are summarized in table 4. No statistically significant differences were found between the east- and west-flank mountains; therefore, the lapse rates were combined into a single mean value for each month. The difference in lapse rates between the valleys and plains was statistically significant in December. Because a difference occurred in only 1 of 12 months, and because at the chosen significance level differences could be incorrectly identified only 10 percent of the time, lapse rates for the valleys and plains were combined and a single value was computed for each month. When the monthly mean values for the combined mountains and the combined valleys and plains were tested, statistically significant differences in mean lapse rate were found for each month. Different lapse rates for minimum air temperature, therefore, are needed in the study area for the mountains and for the valleys and plains.

Table 4.--*Monthly mean lapse rates for minimum air temperature (TLN)*

Stations	Sample size	Lapse rate, in Fahrenheit degrees per 1,000 feet											
		Jan	Feb	Mar	Apr	May	June	July	Aug	Sept	Oct	Nov	Dec
East-flank mountains	8	4.5	4.1	4.5	5.1	5.2	5.8	6.8	6.4	5.5	4.4	4.0	3.7
West-flank mountains	7	4.7 [1]	5.1 [1]	5.6 [1]	4.8 [1]	4.6 [1]	4.6 [1]	5.2 [1]	5.3 [1]	4.7 [1]	3.8 [1]	4.4 [1]	4.9 [1]
Valleys	12	-2.1	-1.2	1.9	1.0	1.9	2.2	.2	-.8	-1.4	-1.6	-1.5	-2.6
Plains	10	-1.5 [1]	.9 [1]	1.6 [1]	.9 [1]	3.2 [1]	2.2 [1]	1.8 [1]	1.5 [1]	1.3 [1]	.7 [1]	.0 [1]	-.6 [2]
Combined mountains	15	4.6	4.5	5.0	5.0	4.9	5.2	6.1	5.9	5.1	4.1	4.2	4.3
Combined valleys and plains	22	-1.8 [2]	.3 [2]	1.8 [2]	.9 [2]	2.5 [2]	2.2 [2]	.9 [2]	.2 [2]	-.2 [2]	-.6 [2]	-.8 [2]	-1.6 [2]

[1] The two preceding values in the column were not significantly different.
[2] The two preceding values in the column were significantly different (at the 0.10 significance level).

The monthly mean lapse rates for minimum air temperature also displayed seasonal variation. In the combined mountains, the lapse rate was smallest in October (4.1 F°/1,000 ft) and largest in July (6.1 F°/1,000 ft). In the combined valleys and plains, the lapse rates ranged from -1.8 F°/1,000 ft in January to 2.5 F°/1,000 ft in May. Unlike lapse rates for maximum and minimum air temperatures in the mountains, the lapse rates for minimum air temperature in the valleys and plains commonly were negative. The negative values indicate that minimum air temperatures commonly will be less at low elevations than at high elevations.

Estimates of daily maximum and minimum air temperatures will be more accurate using monthly lapse rates than using a single lapse rate. However, estimate errors will still occur and might be larger for some months than for others. The coefficient of variation (standard deviation divided by the mean then multiplied by 100) in lapse rate can be used to assess the variability.

The coefficients of variation in lapse rates for maximum air temperature were computed using lapse rates for the combined mountains, valleys, and plains (table 5). The lapse rates for maximum air temperature were moderately variable. The lapse rates were most variable in January (111 percent). The variability decreased to 61 percent in May, then generally increased through the remainder of the year. The period of smallest variability was April through August, when the coefficients of variation were less than 80 percent. Although daily temperature estimates can be obtained using the monthly mean lapse rates, the coefficients of variation indicate that the estimates for some days might be considerably in error.

The coefficients of variation in lapse rates for minimum air temperature were computed for the combined mountains, and for the combined valleys and plains, because the mean lapse rates were significantly different (table 5). The lapse rates for minimum air temperature in the combined mountains displayed less variability than those for maximum air temperature in the combined mountains, valleys, and plains. The large variability in lapse rates for maximum air temperature resulted from the combining of more variable lapse rates from the valleys with less variable lapse rates from the mountains and plains. The lapse rates for minimum air temperature in the mountains were most variable in December (74 percent) and least variable in June (23 percent). The period of least variability was March through August, when the coefficients of variation were less than 40 percent. In the mountains, minimum air temperatures estimated from the mean lapse rates for

Table 5.--*Coefficients of variation in lapse rates for maximum (TLX) and minimum (TLN) air temperatures*

Stations	Lapse rate	Coefficient of variation, in percent											
		Jan	Feb	Mar	Apr	May	June	July	Aug	Sept	Oct	Nov	Dec
Combined mountains, valleys, and plains	TLX	111	108	86	72	61	78	70	66	82	79	85	96
Combined mountains	TLN	48	46	30	24	27	23	30	36	40	53	59	74
Combined valleys and plains	TLN	239	1,937	190	332	160	201	627	1,997	2,911	761	504	234

some days will be moderately in error. The error in the estimates will be least from March through August.

The lapse rates for minimum air temperature in the combined valleys and plains displayed the largest variability. The lapse rates were most variable in September (2,911 percent) and least variable in May (160 percent). The coefficients of variation were large during all months, indicating that minimum temperatures estimated from mean lapse rates could be in error much of the time.

Vegetation

Vegetation was studied in terms of crown cover and rooting depth. Estimates of crown cover are needed for each hydrologic response unit in PRMS. Crown-cover estimates are also needed in the computation of net precipitation. Rooting depth is not a parameter in PRMS but is used to estimate the thickness of the soil-zone reservoir, which in turn is used to determine maximum soil-moisture storage.

Vegetation Crown Cover

PRMS requires two parameters for crown cover: COVDNS for summer conditions and COVDNW for winter conditions. COVDNS can be estimated as the fraction of a hydrologic response unit that is covered by vegetation of all types. COVDNW can be estimated as COVDNS minus the fraction of the hydrologic response unit that is covered by deciduous vegetation. An intimate knowledge of the crown cover within a hydrologic response unit is needed to estimate the percentage of vegetation that is deciduous.

Crown-cover data for the study area were available from several sources. Vegetation surveys have been completed for various purposes by Federal agencies, mining companies, and universities. Depending on the purpose of the preceding vegetation surveys, the level of detail ranged from crown cover by individual plant species to crown cover by all species in a vegetation type. Some of the crown-cover data were more detailed than needed in PRMS. Therefore, the data were summarized in two ways. First, the data were summarized (table 6) as the total crown cover within a vegetation type or dryland crop without regard to growth form such as shrubs, grasses or forbs, or trees. Second, in some applications of PRMS, it might be necessary to know the crown cover by growth form. For example, the estimate of the transmission coefficient for short-wave radiation is based on a relation with tree crown cover; trees also have a greater capacity to retain intercepted precipitation than shrubs or grasses. Therefore, the data were summarized (table 7) as the crown cover within each vegetation type according to growth form: shrubs, grasses and forbs, and trees.

In both summaries, crown cover was categorized by landform and sample statistics were computed. The mean crown cover is the arithmetic mean of the percentages of crown cover, except when only one value of crown cover was reported. The range, standard deviation, and coefficient of variation were provided to aid in assessing the variability in crown cover. The final entry is the sample size (number of observations).

Mean crown cover without regard to growth form (table 6) is most extensive in the riparian-woods type of vegetation (63 percent) and least extensive in the ponderosa-pine type (24 percent). The percentages reflect more favorable growing conditions (thicker soils and greater available moisture) in the riparian-woods type than in the ponderosa-pine type. On the basis of coefficient of variation, crown cover is less variable in the riparian-woods type (6 percent) than in the ponderosa-pine type (71 percent).

Table 6.--*Total crown cover within major vegetation types and dryland crops, by landform*[1]

Vegetation type or dryland crop	Landform	Crown cover				
		Mean (percent)	Range (percent)	Standard deviation (percent)	Coefficient of variation (percent)	Sample size
Mixed grassland (mid and short grasses)	Hills, ridges	37	10-79	21	57	27
	Flood plains, valley floors, alluvial fans, foot slopes.	44	5-96	19	43	83
	Uplands	32	10-79	14	44	71
Big sagebrush-grassland	Hillsides, ridges	33	12-66	14	42	22
	Valley floors, alluvial fans, terraces, foot slopes, benches.	47	10-96	18	38	61
	Uplands	30	12-60	12	40	30
Silver sagebrush-grassland	Valley floors, alluvial fans, terraces, foot slopes.	43	5-66	17	40	22
	Uplands	37	31-60	12	32	8
Greasewood	Valley floors, terraces, ridges.	39	13-60	23	59	5
	Uplands	27	13-60	18	67	6
Ponderosa pine	Foot slopes, hills, uplands.	24	11-60	17	71	21
Riparian woods	Flood plains	63	59-66	4	6	4
Breaks	Breaks	25	12-36	8	32	12
Dryland grain	Alluvial fans, terraces, uplands.	38	24-62	11	29	14
Alfalfa	Alluvial fans, terraces, foot slopes.	45	11-64	16	36	10

[1] Data summarized from the following reports: Consolidation Coal Company (1981b), Kiewit Mining and Engineering Company (1982a), Northern Energy Company, Inc. (1978, 1979), U.S. Bureau of Land Management (1975), U.S. Department of the Interior (1977a,b,c), and VTN Environmental Consultants (1976).

Table 7.--*Crown cover identified by growth form within major vegetation types,*

Vegetation type	Landform	Crown cover of shrubs					Crown cover of grasses and forbs				
		Mean (percent)	Range (percent)	Standard deviation (percent)	Coefficient of variation (percent)	Sample size	Mean (percent)	Range (percent)	Standard deviation (percent)	Coefficient of variation (percent)	Sample size
Mixed grassland (mid and short grasses)	Hills, ridges	2	0-6	2	100	5	56	9-90	32	57	5
	Flood plains, valley floors, alluvial fans, terraces, foot slopes, benches.	4	2-10	3	75	8	55	28-96	22	40	11
	Uplands	7	6-9	1	14	3	56	35-75	20	36	3
Big sagebrush-grassland	Hillsides, ridges.	13	3-28	10	77	5	58	36-69	13	22	5
	Valley floors, alluvial fans, terraces, foot slopes, benches.	18	11-25	5	28	8	32	21-53	13	41	8
	Uplands	23	17-29	6	26	3	40	23-53	15	38	3
Silver sagebrush-grassland	Valley floors, alluvial fans, terraces, foot slopes.	29	22-38	6	21	6	51	37-64	11	22	6
Greasewood	Alluvial fans, terraces.	14	8-22	8	57	3	23	4-49	23	100	3
Ponderosa pine	Foot slopes, hills, uplands.	5	2-8	3	60	3	30	22-42	10	33	3
Riparian woods	Flood plains	8	1-16	11	137	2	59	54-65	8	14	2
Breaks	Breaks	22	14-31	7	32	5	26	19-36	7	27	5

[1] Data summarized from the following reports: Consolidation Coal Company (1981b), Kiewit Mining and U.S. Bureau of Land Management (1975), U.S. Department of the Interior (1977a,b,c), and VTN En-

Mean crown cover with regard to growth form (table 7) also reflects conditions favorable to plant growth. Mean crown cover of shrubs was most extensive in the silver-sagebrush-grassland type (29 percent) and least extensive in the mixed-grassland type on hills and ridges (2 percent). Mean crown cover of grasses and forbs was most extensive in the riparian-woods type (59 percent) and least extensive in the greasewood type (23 percent). Mean crown cover of trees was most extensive in the ponderosa-pine type (14 percent) and least extensive in the riparian-woods type (2 percent). However, the sample sizes were small for both types, which might affect the results.

Crown cover of shrubs was most variable in the riparian-woods type (coefficient of variation of 137 percent) and least variable in the mixed-grassland type on uplands (14 percent). However, only two samples were available for the riparian-woods type and three for the mixed-grassland type. Crown cover of grasses and forbs was most variable in the greasewood type (100 percent) and least variable in the riparian-woods type (14 percent), on the basis of three and two samples, respectively. The variability of crown cover of trees (maximum of 133 percent, minimum of 79 percent) was computed for the greasewood and ponderosa-pine types for

by landform[1]

Crown cover of trees				
Mean (percent)	Range (percent)	Standard deviation (percent)	Coefficient of variation (percent)	Sample size
--	--	--	--	--
--	--	--	--	--
--	--	--	--	--
--	--	--	--	--
--	--	--	--	--
--	--	--	--	--
--	--	--	--	--
6	0-12	8	133	2
14	4-26	11	79	3
2	--	--	--	1
4	--	--	--	1

Engineering Company (1982a), vironmental Consultants (1976).

two and three samples. Only one sample was reported for both the riparian-woods and breaks types. The variability was affected by small sample sizes.

Vegetation Rooting Depths

Soil-profile descriptions commonly provide observations of root occurrence; therefore, reports containing profile descriptions of soils in the study area were reviewed. For each profile description containing root occurrence, the rooting depths observed were recorded along with vegetation, soil texture, and landform. The profile descriptions generally included the deepest roots. In some instances, however, some plant species may have roots that extend to greater depths than the depth of the pit used to describe the profile. Big sagebrush, for example, is known to root to 10 ft or more under favorable soil conditions (Campbell and Harris, 1977, p. 652; Sturges, 1978, p. 89; Tabler, 1964, p. 634). In spite of this limitation, the profile descriptions provide a major source of information.

Data for rooting depths and soil-texture classes, by vegetation type and landform, are summarized in table 8. The computed relative frequency of occurrence of soil texture may provide assistance in estimating physical properties of soils and also in distinguishing between vegetation types when time does not permit extensive fieldwork. A considerable bias may exist owing to the small sample size. Also, site selection for profile descriptions is not random. Rather, sites were selected for their representation of the soil series. Vegetation types, therefore, may occur on soils having textures that were not sampled.

Rooting depths generally agreed with observations made earlier with regard to crown cover. The deepest roots generally occurred in thickest soils with favorable moisture regimes. The roots were deepest in the riparian-woods type (mean depth 48 in.). The rooting depths were shallowest in ponderosa-pine type (mean depth 24 in.) and in the breaks (19 in.). The shallow depths reflect, at least in part, the thin rocky soils. Rooting depths were most variable in the greasewood type and least variable in the riparian-woods type, on the basis of coefficient of variation. The coefficient of variation was 66 percent in the greasewood type on uplands and 19 percent in the riparian-woods type.

Soils

Eight model parameters are directly or indirectly related to physical or hydrologic properties of soils (table 1). Parameters in the daily mode include the maximum snowmelt-infiltration rate of the soil profile at field capacity (SRX), seepage rate from the soil-zone reservoir to the ground-water reservoir (SEP), maximum soil-moisture storage in the soil-zone reservoir (SMAX), and maximum soil-moisture storage in the recharge zone (REMX). Parameters in the storm mode include hydraulic conductivity at the wetting front (KSAT), and the three coefficients PSP, RGF, and DRN.

The parameters can be computed from values of the physical or hydrologic soils properties, if they have been determined. In routine laboratory analysis of soils,

Table 8.--*Rooting depths and soil-texture class occurrence of major vegetation types and*

[in., inches; S, sand; SL, sandy loam; L, loam; SiL, silt loam; Si; silt; SCL, sandy clay loam; CL, clay loam; SC, sandy clay; SiC, silty clay; C, clay; -- indi-

Vegetation type or dryland crop	Landform	Rooting depth				
		Mean (in.)	Range (in.)	Standard deviation (in.)	Coefficient of variation (percent)	Sample size
Mixed grassland (mid and short grasses)	Hillsides, hills, ridges	32	7-50	15	47	27
	Flood plains, valley floors, alluvial fans, foot slopes.	35	12-65	16	46	83
	Uplands	28	5-56	14	50	71
Big sagebrush-grassland	Hillsides, ridges	29	10-40	10	34	22
	Valley floors, alluvial fans, terraces, foot slopes, benches.	41	15-63	14	34	61
	Uplands	38	12-60	10	26	30
Silver sagebrush-grassland	Valley floors, alluvial fans, terraces, foot slopes.	37	18-60	18	49	22
	Uplands	36	31-60	14	39	8
Greasewood	Flood plains, terraces, ridges	39	13-60	23	59	5
	Uplands	27	13-60	18	66	6
Ponderosa pine	Foot slopes, hills, uplands	24	15-35	8	33	21
Riparian woods	Flood plains	48	36-60	9	19	4
Breaks	Breaks	19	10-38	9	47	12
Dryland grain	Alluvial fans, terraces, uplands	39	26-56	9	23	14
Alfalfa	Alluvial fans, terraces, foot slopes	47	28-64	16	34	10

[1] Data summarized from the following reports: Consolidation Coal Company (1981a), Kiewit Mining and (1979), U.S. Bureau of Land Management (1975), Meshnick and others (1977), U.S. Soil Conservation (1982a,b; 1983).

[2] U.S. Department of Agriculture soil-texture class (Hillel, 1980, p. 60); no data were available for

values for some or all of the properties might not have been determined. If values have not been determined by laboratory analysis, they need to be estimated by other means.

SRX and SEP can be computed as one-half the saturated hydraulic conductivity, which is the hydraulic conductivity of saturated soil (Cary, 1984, p. 30). Because SRX is an infiltration parameter, use of the saturated hydraulic conductivity of the A (uppermost) soil horizon might give the most representative result. Similarly, because SEP is a seepage parameter, use of the saturated hydraulic conductivity of the C (lowermost) soil horizon might give the best result.

SMAX and REMX can be computed as the zone thickness multiplied by the available water-holding capacity of each zone. For SMAX, the user specifies the thickness of the soil-zone reservoir--assumed to be the mean rooting depth of the predominant vegetation in the hydrologic response units. For REMX, the user specifies the thickness of the recharge zone, although the thickness of the A and B soil horizons would provide a physically based value. The available water-holding capacity of each zone is the difference in soil moisture at field capacity and at the wilting point (volumetric basis). Soil moisture at field capacity is assumed to be the soil moisture content at one-third bar suction, whereas soil moisture at the wilting point is assumed to be the soil moisture content at 15 bars suction.

dryland crops, by landform[1]

clay loam; SiCL, silty
cates no data]

Soil texture										
Frequency of occurrence by texture class[2] (percent)										
S	SL	L	SiL	Si	SCL	SiCL	CL	SC	SiC	C
--	15	26	4	--	--	33	15	--	--	7
1	4	32	5	4	--	21	17	--	4	12
3	15	36	10	1	--	17	1	--	3	14
--	5	18	9	--	--	59	9	--	--	--
2	3	39	--	--	--	30	10	--	8	8
--	10	46	--	--	3	27	7	--	--	7
--	9	23	18	5	--	31	5	--	--	9
--	24	25	25	--	--	13	13	--	--	--
--	--	--	20	--	--	--	--	--	--	80
--	--	20	--	--	--	20	40	--	20	--
--	14	48	5	--	--	33	--	--	--	--
--	25	25	--	--	--	--	50	--	--	--
--	--	42	8	--	--	--	8	--	42	--
--	14	29	14	14	--	29	--	--	--	--
--	20	20	--	--	30	--	10	10	--	10

Engineering Company (1982b), Schafer and others
Service (1966a,b; 1978), and Westman and Parrish

the loamy sand texture class.

KSAT, PSP, and RGF are used in a form of the Green and Ampt infiltration equation (Dawdy and others, 1972, p. B5-B7; Leavesley and others, 1983, p. 24-25). In this study, these three model parameters were evaluated from the properties of the A soil horizon.

KSAT is not hydraulic conductivity at full saturation, but generally is in the range of 40 to 60 percent of saturated hydraulic conductivity. KSAT can be estimated as one-half of saturated hydraulic conductivity (Bouwer, 1966, p. 732).

PSP can be computed as the product of moisture deficit at field capacity and suction at the wetting front. Substituting soil moisture at saturation minus soil moisture at one-third bar suction for moisture deficit at field capacity, the relation becomes soil moisture at saturation minus soil moisture at one-third bar suction, multiplied by suction at the wetting front. However, data for soil moisture at saturation are not always available in a laboratory analysis and data for suction at the wetting front are not measured directly. Therefore, these properties may need to be computed from other soils-related parameters.

When data for soil moisture at saturation are not available, porosity can be used as a substitute. Porosity is computed as 1 - bulk density/particle density. Bulk density can be determined for either dry or moist soil. Bulk density at one-third bar suction (field capacity) commonly is used for moist soil (U.S. Soil Conservation Service, 1983, p. 603.16, 603.23). The particle density is the mean particle density, which is about 2.65 grams per cubic centimeter.

Suction at the wetting front can be determined from the following equation (Brakenseik, 1977, p. 680):

$$\Psi_f = \frac{3\lambda + 2}{3\lambda + 1}\left(\frac{\Psi_e}{2}\right) \qquad (10)$$

where

Ψ_f = suction at the wetting front, in inches;
λ = pore-size distribution index, dimensionless; and
Ψ_e = suction at air entry, in inches.

The pore-size distribution index (λ) and suction at air entry (Ψ_e) in equation 10 are obtained from soil-desorption data. The pore-size distribution index is the slope of the soil-moisture desorption curve, and suction at air entry is the intercept when the logarithms of relative soil moisture are plotted against the logarithms of suction.

Table 9.--*Summary of the regression analyses of selected prop-*

[Regression equation: $Y = a + bX_1 + cX_2 + dX_3 + eX_4 + fX_5 +$

for explanatory variables are by weight. The coefficient standard error divided by the mean value of the response 100. Abbreviations: g/cm^3, grams per cubic centi- hour. --, variable not

Equation No.	Response variable (Y)	Regression constant (a)	Regression coefficient for indicated explanatory variable				
			(b) Percent sand (X_1)	(c) Percent silt (X_2)	(d) Percent clay (X_3)	(e) Dry bulk density (g/cm^3) (X_4)	(f) Percent organic carbon (X_5)
A	Saturated hydraulic conductivity (in/h)	1.2567	0.0277	--	--	--	--
B	Soil moisture at one-third bar suction (percent by volume)	12.9030	--	0.1857	0.6192	--	--
C	Soil moisture at one-third bar suction (percent by volume)	37.4183	--	.1584	.6712	-15.6915	-1.4331
D	Soil moisture at one-third bar suction (percent by volume)	15.2132	--	--	--	--	-.7654
E	Soil moisture at 15 bars suction (percent by volume)	2.7254	--	--	.5802	--	--
F	Soil moisture at 15 bars suction (percent by volume)	-1.1572	--	--	.1002	--	--
G	Porosity (percent)	54.2856	-.0929	--	-.2184	--	.9817
H	Dry bulk density (g/cm^3)	1.2114	.0025	--	.0058	--	-.0260
I	Bulk density at one-third bar suction (g/cm^3)	1.1491	.0044	--	--	--	-.0434
J	Bulk density at one-third bar suction (g/cm^3)	.1633	.0008	--	-.0069	.8805	--
K	Pore-size distribution index	.2662	--	--	--	--	--
L	Suction at air entry (bars)	-.4380	--	--	--	.2414	--

RGF can be computed as the product of moisture deficit at the wilting point and suction at the wetting front divided by the product of moisture deficit at field capacity and suction at the wetting front. Moisture deficit at the wilting point is soil moisture at saturation minus soil moisture at 15 bars suction. Moisture deficit at field capacity and suction at the wetting front can be determined by the same procedures described for PSP.

DRN is a coefficient for redistribution of moisture from saturated storage to the recharge zone that can be computed as a fraction of saturated hydraulic conductivity. In an earlier study, Cary (1984, p. 34) computed initial values of

erties for undisturbed soil samples

$gX_6 + hX_7 + iX_8$. All percentages

of variation is the regression variable then multiplied by meter; in., inches per significant]

Regression coefficient for indicated explanatory variable--Continued			Regression statistic			
(g)	(h)	(i)				
Percent soil moisture at one-third bar suction (X_6)	Percent soil moisture at 15 bars suction (X_7)	Sampling depth (in.) (X_8)	Sample size	Coefficient of variation (percent)	Multiple coefficient of determination (R^2)	Computed F value
--	-0.1229	-0.0063	104	131	0.46	30
--	--	--	199	28.5	.47	86
--	--	--	199	27.9	.50	48
--	1.7868	--	199	22.3	.69	219
--	--	--	199	34.6	.64	345
--	1.3419	--	199	10.1	.96	2,044
--	--	-.0612	199	10.1	.31	23
--	--	.0016	199	8.3	.33	23
--	--	--	95	8.9	.54	53
--	--	--	95	5.9	.80	120
--	-.0084	--	104	21.7	.36	58
0.0058	--	--	104	100	.54	58

DRN as one-fourth the saturated hydraulic conductivity.

Thus, to enable computation of all eight soils-related model parameters, values for the following physical and hydrologic properties are needed: saturated hydraulic conductivity, soil moisture at one-third bar suction, soil moisture at 15 bars suction, porosity, dry bulk density, bulk density at one-third bar suction, pore-size distribution index, and suction at air entry. Multiple, stepwise linear regression was used to develop 12 estimating equations for the response (dependent) variables described above (table 9). The explanatory (independent) variables were properties commonly determined as part of a soil sample analysis.

The equations were developed using unpublished soil data from a small watershed study conducted by the U.S. Geological Survey in southeastern Montana and data from reports of Williams and others (1973) and the U.S. Soil Conservation Service (1978). Data from the soil samples included different sampling depths, which represented all three soil horizons, and several texture classes. Texture class, sample size, and relative frequency of occurrence are given in table 10. The most common soil was loam. Sand, silt, and sandy clay were not represented in the data.

Data for most physical and hydrologic properties were reported for 199 samples (table 9). Exceptions were saturated hydraulic conductivity (104 samples), bulk density at one-third bar suction (95 samples), pore-size distribution index (104 samples), and suction at air entry (104 samples). Soil moisture at saturation, which is needed to compute relative soil moisture and thus the pore-size distribution index and suction at air entry, was reported for 104 samples. Soil moisture at 6 values of suction was reported for only 39 samples. It was reported at 2 values of suction (one-third and 15 bars) for all 199 samples. A comparison of values of the pore-size distribution index and suction at air entry determined from six points to values determined from two points indicated that reasonable estimates could usually be obtained using two points.

Table 10.--*Soil-texture classes represented in the soil samples used in the analyses*

Texture class[1]	Sample size	Relative frequency (percent)
Sand	0	0
Loamy sand	7	3.5
Sandy loam	32	16.1
Loam	62	31.2
Silt loam	17	8.5
Silt	0	0
Sandy clay loam	15	7.5
Silty clay loam	13	6.5
Clay loam	24	12.1
Sandy clay	0	0
Silty clay	6	3.0
Clay	23	11.6
Total	199	100.0

[1] U.S. Department of Agriculture soil-texture class (Hillel, 1980, p. 60).

When a useful estimating equation could be obtained from a different combination of explanatory variables, it was included (table 9). Thus, equations are available for some properties. Where multiple equations are shown, they are reported in increasing order of the coefficient of determination. Variables were added until incremental increases in the coefficient of determination failed to exceed about 5 percent.

The regression statistics are summarized in table 9. The coefficient of variation is provided instead of the standard error to permit comparisons between the regressions. The coefficient of determination measures the quantity of variation in the response variable that is accounted for by variation in the explanatory variables. The computed F statistic is provided, from which the significance of the regression can be determined. All equations in table 9 are significant at the 0.10 significance level.

About one-half of the variation in saturated hydraulic conductivity (coefficient of determination of 0.46) was accounted for by the explanatory variables. However, large errors in the estimate can occur when equation A in table 9 is used. The coefficient of variation was 131 percent for saturated hydraulic conductivity.

If soil-moisture (percent by weight) and bulk-density data are available, soil moisture (percent by volume) can be computed. Otherwise, it can be estimated from equations B-F in table 9. Fair estimates of soil moisture at one-third bar suction can be obtained using equation B and soil-texture data (coefficient of variation of 28.5 percent, coefficient of determination of 0.47). Marginal improvement in accuracy is indicated in equation C using soil texture, dry bulk density, and percentage organic carbon (coefficient of variation of 27.9, coefficient of determination of 0.50). More accurate estimates can be obtained from equation D if organic carbon and soil moisture at 15 bars suction (by weight) are available (coefficient of variation of 22.3 percent, coefficient of determination of 0.69). Soil moisture at 15 bars suction (percent by volume) can be estimated using equation E from the percentages of clay (coefficient of determination of 0.64), but errors in excess of 30 percent (coefficient of variation of 34.6 percent) can be expected. Better estimates are possible (equation F) if the percentage soil moisture at 15 bars suction (by weight) is available (coefficient of variation of 10.1 percent, coefficient of determination of 0.96). This equation could be used if bulk density at one-third bar suction was not available to convert weight to volume.

Porosity can be computed if measured or estimated values of bulk density are available. Otherwise, estimates can be made using equation G in table 9 with data for soil texture, percentage organic carbon, and sampling depth (coefficient of variation of 10.1 percent, coefficient of determination of 0.31).

Three equations were developed for bulk density--one for dry bulk density and two for bulk density at one-third bar suction. Reasonable estimates of dry bulk density can be determined from equation H in table 9 using percentages of sand, clay, and organic carbon, and the sampling depth. Although the coefficient of determination was 0.33, the coefficient of variation was small (8.3 percent). Bulk density at one-third bar suction can be estimated from equation I using only the percentages of sand and organic carbon (coefficient of variation of 8.9 percent, coefficient of determination of 0.54). Better estimates can be obtained from equation J if the percentages of sand and clay and the dry bulk density are known (coefficient of variation of 5.9 percent, coefficient of determination of 0.80).

Only one explanatory variable was significant in explaining the variation in the pore-size distribution index (coefficient of determination of 0.36). Estimates can be made using equation K in table 9 and the percentage soil moisture at 15 bars suction (by weight).

About one-half of the variation in suction at air entry (coefficient of determination of 0.54) was accounted for by the explanatory variables. However, large errors in the estimate can occur when equation L in table 9 is used. The coefficient of variation was 100 percent for suction at air entry.

Regression model estimates of the soil properties were compared to measured values obtained from Schafer and others (1979) and Williams and others (1973), and mean relative errors were computed (table 11). Although the sample size was not large, the mean relative errors between measured and estimated values generally followed the hierarchy of variability described by Warrick and Nielson (1980, p. 326-327). Estimates of dry bulk density had the least error (mean relative error of 3 percent). Estimates of soil moisture at one-third and 15 bars suction (percent by volume), porosity, bulk density at one-third bar suction, and the pore-size distribution index had moderate errors (mean relative errors of 8 to 39 percent). Estimates of suction at air entry were large (mean error of 58 percent), and estimates of saturated hydraulic conductivity were very large (mean error of 546 percent).

Table 11.--*Relative error between measured soil properties and estimates made using the regression equations from table 9*

[g/cm^3, grams per cubic centimeter; in/h, inches per hour]

Equation No. (table 9)	Response variable	Sample size	Mean relative error[1] (percent)
A	Saturated hydraulic conductivity (in/h)	10	546
B	Soil moisture at one-third bar suction (percent by volume)	10	31
C	Soil moisture at one-third bar suction (percent by volume)	9	31
D	Soil moisture at one-third bar suction (percent by volume)	9	26
E	Soil moisture at 15 bars suction (percent by volume)	9	39
F	Soil moisture at 15 bars suction (percent by volume)	9	17
G	Porosity (percent)	9	8
H	Dry bulk density (g/cm^3)	10	3
I	Bulk density at one-third bar suction (g/cm^3)	10	12
J	Bulk density at one-third bar suction (g/cm^3)	9	26
K	Pore-size distribution index	9	26
L	Suction at air entry (bars)	9	58

[1] Relative error = $\frac{(\text{measured} - \text{estimated})}{(\text{measured})} \times 100$.

Subsurface Flow and Base Flow

Computation of subsurface flow requires one or two parameters, depending on the option selected, whereas computation of base flow requires one parameter. Subsurface flow (RAS) is computed as a linear or nonlinear function of the volume in storage (RES) in the subsurface reservoir. Only the linear option was considered in this study owing to the conceptual nature of the nonlinear function and the uncertainty about estimation of the parameter. The routing coefficient in the linear function (RCF) needs to be estimated. RCF, which can be estimated by hydrograph separation and recession analysis (Leavesley and others, 1983, p. 32), is given by:

$$RCF = - \ln Ks \tag{11}$$

where

Ks = slope of the subsurface-flow recession when flow is plotted on a logarithmic scale.

Base flow (BAS) is computed as a linear function of storage (GW). The routing coefficient in the function (RCB) can be obtained from an analysis of the base-flow recession. RCB is shown by Leavesley and others (1983, p. 34) to be:

$$RCB = - \ln K \tag{12}$$

where

K = the recession constant in the following recession function:

$$q_t = q_o K^t \tag{13}$$

where

q_t = streamflow at time t, in cubic feet per second; and
q_o = streamflow at time zero, in cubic feet per second.

B.S. Barnes (in Hall, 1968, p. 976) reported that the recession curves of surface, subsurface, and base flow could all be described by this function.

Alternately, a function of the form:

$$q_t = q_o \exp(-bt) \tag{14}$$

can be used where q_o, q_t, and t are as defined above, and exp (-b) = K. In this instance, the linear subsurface-flow and base-flow routing coefficients are given as:

$$RCF = b_s, \text{ and} \tag{15}$$

$$RCB = b_b, \tag{16}$$

where, after hydrograph separation,

b_s = slope of the subsurface-flow recession, and
b_b = slope of the base-flow recession.

Many small streams in arid or semiarid regions are either ephemeral or intermittent. Commonly, spring and summer storms result in little or no base flow. The streamflow hydrograph then is composed primarily of surface and subsurface flow. Flow resulting from the storms is preceded by no flow, and the recession lasts but a few days, then recedes to no flow.

Surface flow on forest and rangeland watersheds is not common in the study area. Its occurrence is associated with intense summer storms or runoff over frozen ground. In its absence, the hydrograph will consist of subsurface and (or) base flow.

The surface-water records for Montana, western North Dakota, and Wyoming were reviewed. Daily streamflow hydrographs for drainage areas of 100 mi^2 or less in plains or foothills were obtained from the U.S. Geological Survey (1955-58 and 1960, 1966-70, 1971-74, 1975-81a, and 1975-81b). The hydrographs used were simple (a single rising and receding limb), with relatively long recession periods (1 week or longer), and began with spring snowmelt and continued through the fall. Hydrographs that appeared to represent flow over frozen ground were excluded. The locations of 21 streamflow-gaging stations used in the analysis are shown in figure 8. The corresponding station name and number, drainage area, and elevation are given in table 12.

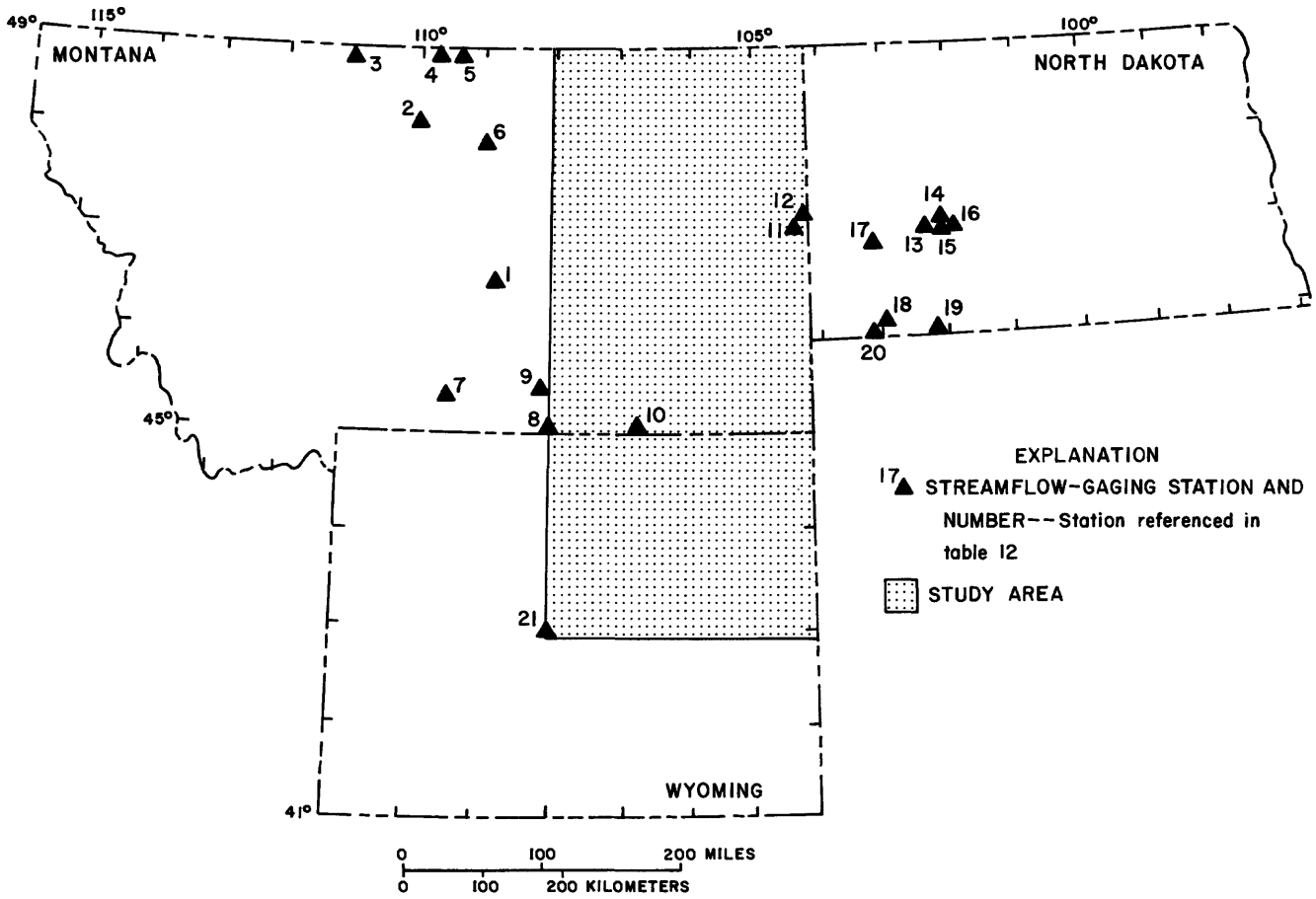

Figure 8.--Location of streamflow-gaging stations used in determining subsurface-flow and base-flow recession.

Many of the surface-water records reviewed were from gaging stations installed during 1971-78, primarily as part of coal-related studies. Of the remaining gaging stations, few had been operated for long periods. Several were not used in this analysis because of an insufficient period of record. Gaging stations were included in the analysis if six or more simple hydrographs could be identified. Also, those with fewer hydrographs were included if a satisfactory range in peak flows was represented.

Table 12.--*Streamflow-gaging stations used in the study of subsurface-flow and base-flow recession*

[Station name: numbers in parentheses correspond to location numbers in figure 8]

Station name	Station No.	Drainge area (square miles)	Elevation above sea level (feet)	Mean subsurface-flow recession constant ($\bar{b}_s$) (cubic feet per second per day)	Mean base-flow recession constant ($\bar{b}_b$) (cubic feet per second per day)
Halfbreed Creek near Klein, Mont. (1)	06126470	53.2	3,330	0.60	0.90
Boxelder Creek near Rocky Boy, Mont. (2)	06137570	48.2	3,225	.61	.91
Sage Creek near Whitlash, Mont. (3)	06137580	7.2	3,900	.53	.93
Woodpile Coulee near international boundary, Mont. (4)	06150000	60.2	2,740	.63	.89
Lyons Creek at international boundary, Mont. (5)	06151000	66.7	2,800	.61	.84
Little Peoples Creek near Hays, Mont. (6)	06154410	13.0	3,760	.58	.95
Willow Creek near Boyd, Mont. (7)	06211500	53.3	4,260	.52	.94
Soap Creek near St. Xavier, Mont. (8)	06287500	98.3	3,250	.64	.95
Beauvais Creek near St. Xavier, Mont. (9)	06288200	100.0	3,350	.61	.93
East Trail Creek near Otter, Mont. (10)	06307560	31.3	3,570	.55	.87
Hay Creek near Wibaux, Mont. (11)	06336515	11.4	2,640	.52	.85
Little Beaver Creek near Wibaux, Mont. (12)	06336545	96.2	2,555	.63	.90
Elm Creek near Golden Valley, N. Dak. (13)	06339490	82.0	1,915	.54	.90
Coyote Creek near Zap, N. Dak. (14)	06339550	5.2	1,810	.54	.85
Brush Creek near Beulah, N. Dak. (15)	06339560	22.0	1,948	.50	.91
West Branch Otter Creek near Beulah, N. Dak. (16)	06340200	26.5	1,975	.43	.88
North Creek near South Heart, N. Dak. (17)	06342970	40.8	2,470	.39	.77
Coal Bank Creek near Havelock, N. Dak. (18)	06349930	70.0	2,505	.46	.89
Timber Creek near Bently, N. Dak. (19)	06352400	100.0	2,280	.49	.91
Buffalo Creek tributary near Gascoyne, N. Dak. (20)	06355310	15.7	2,725	.38	.91
Dry Creek near Bonneville, Wyo. (21)	06256900	52.6	5,010	.63	.83

Human activities, in addition to all the physiographic, geologic, vegetation, soils, and climatic factors, can affect hydrograph characteristics. Cultivation, diversion for irrigation, and storage in stock reservoirs are some important factors in the region. Because separation of drainage basins relatively unaffected by human activities would be difficult, if not impossible, land use was ignored in the selection of discharge data.

The hydrographs were plotted on semilogarithmic paper. The base-flow recession constant (the slope) was estimated from the tail of the recession curve. The base-flow recession curve was then extended backward, beneath the total hydrograph. The day that the base-flow curve began to deviate substantially from the total recession curve was selected as the time of peak base flow. A straight line was drawn from the streamflow on the day prior to the beginning of the rise to the peak streamflow. The ordinates of the base-flow hydrograph were subtracted from the ordinates of the total hydrograph, and the residuals were plotted.

The segment of the residual plot that trended as a straight line (or nearly so) was considered to be the recession of subsurface flow, and the subsurface-flow recession constant was estimated. In some instances, such as during snowmelt or when streamflow was the result of frontal storms, the remaining hydrograph including the peak plotted as a straight line. This part of the hydrograph was interpreted to be subsurface flow. In other instances the peak, and occasionally the flow 1 or 2 days after the peak, deviated from a straight line. The subsurface-flow recession constant was determined from the hydrograph beginning at the inflection of the recession curve. Such hydrographs generally were associated with summer storms.

When streamflow was preceded by no flow but the tail of the recession was relatively long (1 week or longer), the same procedure was followed, except that the line defining base flow under the rising limb was extrapolated beginning with

zero flow. When the rise was not preceded by flow, and when the recession lasted but a few days, returning to no flow, no base flow was assumed. The hydrograph then consisted of surface and subsurface flow.

The mean values of the recession coefficients were computed for the 21 gaging stations retained in the analysis. Multiple, stepwise linear regressions were computed, with the mean subsurface-flow recession constants ($\bar{b}_s$) and the mean base-flow recession constant ($\bar{b}_b$) as response variables. The explanatory variables included latitude, longitude, and elevation of the gaging station; drainage area upstream from the gaging station; mean annual precipitation at the gaging station nearest the basin; mean annual streamflow (inches per square mile) at the gaging station; and ratio of mean annual streamflow to mean annual precipitation.

Sixty percent of the variation in the subsurface-flow recession constant was explained by two explanatory variables--longitude and drainage area of the gaging station. The resulting estimating relation is:

$$b_s = 4.08 - 0.0314 \text{ (longitude)} - 0.0023 \text{ (drainage area)} \quad (17)$$

A satisfactory relation was not obtained for the base-flow recession constant. Therefore, the data were reanalyzed after deletion of data from 10 gaging stations (8 in North Dakota and 2 in extreme eastern Montana). Of the remaining gaging stations, 10 were in Montana and 1 was in Wyoming. A significant relation was found between the base-flow recession constant and the variables of mean annual streamflow and mean annual precipitation. Sixty-three percent of the variation in the base-flow recession constant was explained by the explanatory variables. The final estimating relation is:

$$b_b = 0.2189 - 0.0120 \text{ (mean annual streamflow)} - 0.0068 \text{ (mean annual precipitation)} \quad (18)$$

The regression equations can be used to obtain initial estimates of the recession constants when site data are not available. The subsurface-flow routing coefficient is equal to the estimated value of b_s, and the base-flow routing coefficient is equal to the estimated value of b_b.

SUMMARY

Estimation techniques were developed for selected parameters in the U.S. Geological Survey's Precipitation-Runoff Modeling System (PRMS). The results of this study are applicable to the plains and foothills of eastern Montana and northeastern Wyoming.

Values of CTS (air-temperature coefficient) and CTX (air-temperature correction coefficient) in a potential evapotranspiration equation were estimated at points by kriging. CTS and CTX displayed significant changes (trend) east and north from the southwest corner of the study area. Values at each climatological station were corrected for the trend by subtracting an estimate of the mean value. CTS and CTX displayed anisotropy; their semivariograms, therefore, were functions of distance and direction. The radius of influence for both coefficients was 68 mi. Linear theoretical semivariograms were selected to represent the empirical semivariograms, and each semivariogram included a nugget at the origin. Maps were constructed that displayed lines of equal value of the coefficients and the associated error. CTS decreased from 0.0140 $°F^{-1}$ in the southwest corner of the study area to 0.0120 $°F^{-1}$ near the northern boundary. CTX increased from 14.5 °F in the southwest corner to about 18.5 °F near the northern boundary. The associated error in the estimates was greater for CTX than for CTS, but did not exceed 4.0 percent of the estimated value.

Monthly mean lapse rates for maximum (TLX) and minimum (TLN) air temperatures were computed, then statistically tested between the east-flank and west-flank mountains, the major river valleys, and the plains. The results of tests for lapse rates were different for maximum and minimum air temperatures. For maximum air temperature, differences in lapse rates between locations were not statistically significant, and all lapse rates were combined. For minimum air temperature, differences in lapse rates were statistically significant between the combined mountains and the combined valleys and plains. Thus, in the study area, a single monthly mean lapse rate can be used for maximum air temperature. However, for minimum air temperature, the monthly mean lapse rate needs to be different for the mountains and for the valleys and plains.

The monthly mean lapse rates displayed seasonal variation. The monthly mean lapse rate for maximum air temperature was smallest in January (3.2 F°/1,000 ft) and largest in April and May (5.3 F°/1,000 ft). In the combined mountains, the monthly mean lapse rate for minimum air temperature was smallest in October (4.1 F°/1,000 ft) and largest in July (6.1 F°/1,000 ft). In the combined valleys and plains, the monthly mean lapse rates for minimum air temperature ranged from -1.8 F°/1,000 ft in January to 2.5 F°/1,000 ft in May. The monthly mean lapse rates for minimum air temperatures in the combined valleys and plains commonly were negative indicating that, in some months, minimum air temperatures are less at low elevations than at high elevations.

Although daily maximum and minimum air temperatures can be estimated from the lapse rates, the estimates will be in error. Lapse rates for maximum air temperature were most variable in January (111 percent) and least variable in May (61 percent). Lapse rates for minimum air temperature in the mountains displayed the most variability in December (74 percent) and the least variability in June (23 percent). Lapse rates for minimum air temperature in the valleys and plains displayed the largest variability (2,911 percent) in September and the least variability in May (160 percent).

Estimates of vegetation crown cover are used directly in PRMS as parameters--summer crown cover (COVDNS) and winter crown cover (COVDNW). Crown-cover data were extracted from reports describing previous vegetation surveys in the study area. Two summaries were prepared. First, the data were summarized as total crown cover in a vegetation type or dryland crop without regard to growth form. Second, the data were summarized as crown cover by growth form (shrubs, grasses and forbs, and trees).

In the first summary, the vegetation type with the greatest crown cover had the least variability, whereas the type with the least crown cover had the most variability. Mean crown cover was the most extensive (63 percent) and the least variable (coefficient of variation of 6 percent) in the riparian-woods type of vegetation. Mean crown cover was the least extensive (24 percent) and the most variable (coefficient of variation of 71 percent) in the ponderosa-pine type.

In the second summary, the results, which differed from the first summary, might have been affected by small sample sizes. The largest sample size for crown cover of trees was three. Mean crown cover of shrubs was most extensive (29 percent) in the silver-sagebrush-grassland type and least extensive (2 percent) in the mixed-grassland type on hills and ridges. The crown cover of shrubs was most variable (coefficient of variation of 137 percent) in the riparian-woods type and least variable (coefficient of variation of 14 percent) in the mixed-grassland type on uplands. Crown cover of grasses and forbs was most extensive (59 percent) and least variable (coefficient of variation of 14 percent) in the riparian-woods type. Crown cover of grasses and forbs was least extensive (23 percent) and most variable (coefficient of variation of 100 percent) in the greasewood type.

Information on vegetation rooting depth is used to estimate the thickness of the soil-zone reservoir. Rooting depths were obtained from soil-profile descriptions of previous studies. Statistics were computed by major vegetation type and landform. The rooting depths were deepest in the riparian-woods type of vegetation (mean of 48 in.) and shallowest in the ponderosa-pine type (mean of 24 in.) and in the breaks (mean of 19 in.). The rooting depths were most variable in the grease-

wood type (coefficient of variation of 66 percent) and least variable in the riparian-woods type (coefficient of variation of 19 percent).

Estimating equations were developed between the physical and hydrologic properties of soils to which PRMS parameters are related and the properties of soils that commonly are measured. The parameters are maximum snowmelt-infiltration rate of the soil profile at field capacity (SRX), seepage rate from the soil-zone reservoir to the ground-water reservoir (SEP), maximum soil-moisture storage in the soil-zone reservoir (SMAX), maximum soil-moisture storage in the recharge zone (REMX), hydraulic conductivity at the wetting front (KSAT), a coefficient that is the product of moisture deficit at field capacity and suction at the wetting front (PSP), a coefficient that is the product of moisture deficit at wilting point and suction at the wetting front divided by the product of moisture deficit at field capacity and suction at the wetting front (RGF), and a coefficient for redistribution of moisture from saturated storage to the recharge zone (DRN). The physical and hydrologic properties were saturated hydraulic conductivity, soil moisture at one-third bar suction (percent by volume), soil moisture at 15 bars suction (percent by volume), porosity, dry bulk density, bulk density one-third bar suction, pore-size distribution index, and suction at air entry.

Multiple, stepwise linear regression was used to develop 12 estimating equations. One equation was developed for saturated hydraulic conductivity. About one-half of the variation in saturated hydraulic conductivity is accounted for by the explanatory variables (coefficient of determination of 0.46). However, the coefficient of variation is large (131 percent), indicating that errors in the estimates can be large.

Soil moisture at one-third bar suction can be estimated from any of three equations, whereas soil moisture at 15 bars suction can be estimated from either of two equations. Fair estimates can be obtained from soil-texture data (coefficient of variation of 28.5 percent, coefficient of determination of 0.47), but more accurate estimates can be obtained if organic carbon and soil moisture at 15 bars suction (by weight) are available (coefficient of variation of 22.3 percent, coefficient of determination of 0.69). Soil moisture at 15 bars suction can be estimated from only knowledge of the percentage of clay (coefficient of variation of 34.6 percent, coefficient of determination of 0.64). A better estimate is possible if soil moisture at 15 bars suction (by weight) is included (coefficient of variation of 10.1 percent, coefficient of determination of 0.96).

Porosity can be estimated from one equation. Porosity was related to the four explanatory variables of percentages of sand, clay, and organic carbon, and the sampling depth (coefficient of variation of 10.1 percent, coefficient of determination of 0.31).

Dry bulk density can be estimated from one equation, whereas bulk density at one-third bar suction can be estimated from one of two equations. Reasonable estimates of dry bulk density can be obtained (coefficient of variation of 8.3 percent), even though only one-third of the variation was accounted for by the explanatory variables (coefficient of determination of 0.33). Estimates for bulk density at one-third bar suction can be obtained if percentages of sand and organic carbon are available (coefficient of variation of 8.9 percent, coefficient of determination of 0.54). Better estimates can be obtained if the percentages of sand and clay and the dry bulk density are used (coefficient of variation of 5.9 percent, coefficient of determination of 0.80).

The remaining physical and hydrologic properties can be estimated from one equation for each property. The pore-size distribution index can be estimated with the explanatory variable of percentage soil moisture at 15 bars suction (by weight). However, only about one-third (coefficient of determination of 0.36) of the variation is accounted for by the explanatory variable. About one-half of the variation in suction at air entry is accounted for by the explanatory variables (coefficient of determination of 0.54). However, the coefficient of variation is large (100 percent), indicating that errors in the estimates can be large.

The subsurface-flow routing coefficient (RCF) and the base-flow routing coefficient (RCB) are related to computed recession constants of a hydrograph.

Subsurface-flow and base-flow recession constants were determined by hydrograph separation. The hydrographs used were from 21 streamflow-gaging stations on Montana, North Dakota, or Wyoming streams with drainage areas of 100 mi^2 or less. Mean values were computed for the subsurface-flow recession constant ($\bar{b}_s$) and the base-flow recession constant ($\bar{b}_b$) at each gaging station.

Estimating equations for the mean values of the recession constants were developed by linear regression. The subsurface-flow recession constant can be estimated from an equation relating the constant to longitude and drainage area of the gaging station. The two variables explain 60 percent of the variation in the subsurface-flow recession constant. A satisfactory estimating equation was not found for the base-flow recession constant when data from all gaging stations were used. After data from 10 gaging stations (8 in North Dakota and 2 in Montana) were removed and the data were reanalyzed, a significant relation was found between the base-flow recession constant and the explanatory variables of mean annual streamflow and mean annual precipitation. The two variables explain 63 percent of the variation in the recession constant.

REFERENCES CITED

Bouwer, Herman, 1966, Rapid field measurement of air entry value and hydraulic conductivity of soil as significant parameters in flow system analysis: Water Resources Research, v. 2, no. 4, p. 729-738.

Brakenseik, D.L., 1977, Estimating the effective capillary pressure in the Green and Ampt infiltration equation: Water Resources Research, v. 13, no. 3, p. 680-682.

Campbell, G.S., and Harris, G.A., 1977, Water relations and water use patterns for *Artemisia tridentata* Nutt. in wet and dry years: Ecology, v. 58, no. 3, p. 652-659.

Cary, L.E., 1984, Application of the U.S. Geological Survey's precipitation-runoff modeling system to the Prairie Dog Creek basin, southeastern Montana: U.S. Geological Survey Water-Resources Investigations Report 84-4178, 95 p.

Consolidation Coal Company, 1981a, Surface mining permit application, CX Ranch Mine [Montana], volume 9, Soils baseline inventory: Sheridan, Wyo., 176 p.

_____1981b, Surface mining permit application, CX Ranch Mine [Montana], volume 13, Vegetation inventory: Sheridan, Wyo., 284 p.

David, M., 1977, Developments in geomathematics 2, geostatistical ore reserve estimation: Amsterdam, Elsevier Scientific Publishing Co., 364 p.

Dawdy, D.R., Lichty, R.W., and Bergman, J.M., 1972, A rainfall-runoff simulation model for estimation of flood peaks for small drainage basins: U.S. Geological Survey Professional Paper 506-B, 28 p.

Hall, F.R., 1968, Flow recessions--A review: Water Resources Research, v. 4, no. 5, p. 973-983.

Hillel, Daniel, 1980, Fundamentals of soil physics: New York, Academic Press, 413 p.

Jensen, M.E., Robb, D.C.N., and Franzoy, C.E., 1969, Scheduling irrigations using climate-crop-soil data: National Conference on Water Resources Engineering of the American Society of Civil Engineers, New Orleans, La., Feb. 3-5, 20 p.

Keefer, W.R., 1974, Geologic map of the Northern Great Plains: U.S. Geological Survey Open-File Report 74-50, 1 sheet, scale 1:1,000,000.

Kiewit Mining and Engineering Company, 1982a, Surface coal mining permit application, Wolf Mountain Mine [Montana], volumes 8 and 9, Vegetation survey: Sheridan, Wyo., 820 p.

_____1982b, Surface coal mining permit application, Wolf Mountain Mine [Montana], volume 11, Soil survey and land use: Sheridan, Wyo., 205 p.

Leavesley, G.H., 1973, A mountain watershed simulation model: Fort Collins, Colorado State University, unpublished Ph.D. dissertation, 174 p.

Leavesley, G.H., Lichty, R.W., Troutman, B.M., and Saindon, L.G., 1981, A precipitation-runoff modeling system for evaluating the hydrologic impacts of energy resources development: 49th Annual Western Snow Conference Proceedings, St. George, Utah, p. 65-76.

_____1983, Precipitation-runoff modeling system--User's manual: U.S. Geological Survey Water-Resources Investigations Report 83-4238, 207 p.

McCuen, R.H., and Snyder, W.M., 1986, Hydrologic modeling, statistical methods and applications: Englewood Cliffs, N.J., Prentice-Hall, 568 p.

Meshnick, J.C., Smith, J.H., Gray, L.G., Peterson, R.F., Gentz, D.H., and Smith, Ralph, 1977, Soil survey of Big Horn County area, Montana: Bozeman, Mont., U.S. Soil Conservation Service and U.S. Bureau of Indian Affairs, 223 p.

National Oceanic and Atmospheric Administration, 1972-81a, Climatological data, Montana: published monthly.

_____1972-81b, Climatological data, Wyoming: published monthly.

Northern Energy Company, Inc., 1978, Environmental baseline study, Spring Creek Project [Montana], volumes 1 and 2: Portland, Oreg., 752 p.

_____1979, Spring Creek Mine vegetation monitoring program [Montana]: Portland, Oreg., 122 p.

Northern Great Plains Resources Program, 1974, Effects of coal development in the Northern Great Plains: Denver, Colo., U.S. Department of the Interior, 150 p.

Overton, D.E., and Meadows, M.E., 1976, Stormwater modeling: New York, N.Y., Academic Press, 358 p.

Schafer, W.M., Nelson, G.A., Dollhopf, D.J., and Temple, K., 1979, Soil genesis, hydrological properties, root characteristics and microbial activity of 1- to 50-year old strip-mine spoils: U.S. Department of Agriculture, Science and Education Administration, and U.S. Environmental Protection Agency EPA-600/7-79-100, 211 p.

Scott, A.G., 1984, Analysis of characteristics of simulated flows from small surface-mined and undisturbed Appalachian watersheds in the Tug Fork basin of Kentucky, Virginia, and West Virginia: U.S. Geological Survey Water-Resources Investigations Report 84-4151, 169 p.

Skrivan, J.A., and Karlinger, M.R., 1980, Semivariogram estimation and universal kriging program: U.S. Geological Survey computer contribution, 98 p.

Sturges, D.L., 1978, Hydrologic relations of sagebrush lands: Logan, Utah, Sagebrush Ecosystem Symposium, April 27-28, p. 86-100.

Tabler, R.D., 1964, The root system of *Artemisia tridentata* at 9,500 feet in Wyoming: Ecology, v. 45, no. 3, p. 633-636.

U.S. Bureau of Land Management, 1975, Resource and potential reclamation evaluation, Otter Creek study site, Otter Creek coalfield, Montana: EMRIA Report 1, 200 p.

U.S. Department of the Interior, 1977a, Resource and potential reclamation evaluation, Bear Creek study area, West Moorhead coalfield, Montana: EMRIA Report 8, 259 p.

_____1977b, Resource and potential reclamation evaluation, Hanging Woman Creek study area [Montana]: EMRIA Report 12, 309 p.

_____1977c, Resource and potential reclamation evaluation, White Tail Butte study area, Wyoming: EMRIA Report 13, 112 p.

U.S. Geological Survey, 1955-58 and 1960, Surface water supply of the Missouri River basin above Sioux City, Iowa, part 6-A: U.S. Geological Survey Water-Supply Papers 1389, 1439, 1509, 1559, and 1709.

_____1966-70, Surface water supply of the United States, Missouri River basin above Williston, North Dakota, Part 6, Volume 1: U.S. Geological Survey Water-Supply Paper 2116, 835 p.

_____1971-74, Water resources data for Montana, Part 1, Surface water records: Helena, Mont., U.S. Geological Survey reports, issued annually.

_____1975-81a, Water resources data for Montana: Helena, Mont., U.S. Geological Survey Water-Data Reports 75-1 through 81-1, issued annually.

_____1975-81b, Water resources data for North Dakota: Bismarck, N. Dak., U.S. Geological Survey Water-Data Reports 75-2 through 81-2, issued annually.

U.S. Soil Conservation Service, 1966a, Soil survey laboratory data and descriptions for some soils of Montana: Soil Survey Investigations Report 7, 159 p.

_____1966b, Soil survey laboratory data and descriptions for some soils of Wyoming: Soil Survey Investigations Report 8, 97 p.

_____1978, Soil survey laboratory data and descriptions for some soils of Wyoming: Soil Survey Investigations Report 32, 145 p.

_____1983, National soils handbook: Washington, D.C., U.S. Department of Agriculture, 619 p.

U.S. Weather Bureau, 1954, Climatic summary of the United States, Supplement for 1931 through 1952, Climatography of the United States No. 11-42, Wyoming: Washington, D.C., U.S. Government Printing Office, 44 p.

_____1955, Climatic summary of the United States, Supplement for 1931 through 1952, Climatography of the United States No. 11-20, Montana: Washington, D.C., U.S. Government Printing Office, 60 p.

_____1965a, Climatic summary of the United States, Supplement for 1951 through 1960, Climatography of the United States No. 86-20, Montana: Washington, D.C., U.S. Government Printing Office, 81 p.

_____1965b, Climatic summary of the United States, Supplement for 1951 through 1960, Climatography of the United States No. 86-42, Wyoming: Washington, D.C., U.S. Government Printing Office, 77 p.

VTN Environmental Consultants, 1976, Spring Creek Coal Company, Environmental baseline study [Montana]: v. 1 and 2, various pagination.

Warrick, A.W., and Nielson, D.R., 1980, Spatial variability of soil physical properties in the field, Chapter 13 *of* Hillel, Daniel, Applications of soil physics: New York, N.Y., Academic Press, p. 319-335.

Weeks, J.B., Leavesley, G.H., Welder, F.A., and Saulnier, G.J., Jr., 1974, Simulated effects of oil-shale development on the hydrology of Piceance basin, Colorado: U.S. Geological Survey Professional Paper 908, 83 p.

Weisner, C.J., 1970, Hydrometeorology: London, Chapman and Hall, Ltd., 232 p.

Westman, G.H., and Parrish, L.M., eds., 1982a, Resource and potential reclamation evaluation, Pumpkin Creek study area [Montana]: U.S. Bureau of Reclamation EMRIA Report 21-71, 64 p.

_____1982b, Resource and potential reclamation evaluation, Rattlesnake Butte study area, North Dakota: U.S. Bureau of Reclamation EMRIA Report 22-78, 44 p.

_____1983, Resource and potential reclamation evaluation, Prairie Dog Creek study area, Montana: U.S. Bureau of Reclamation EMRIA Report 21-78, 27 p.

Williams, T.T., Koob, R.L., and Rechard, Paul, coordinators, 1973, Surface and groundwater problems associated with potential strip-mine sites: U.S. Environmental Protection Agency Grant No. R-803727, 800 p.